13C-180

DEPARTMENT OF PHYSICS
University of Southern California
Los Angeles, California 90007

Master

USC-136-150

PASSAGE OF CHARGED PARTICLES THROUGH MATTER*

by

Hans Bichsel†
Department of Physics
University of California
Berkeley, California

July 1969

136

---

* This work was supported by Public Health Service Grant No. CA-08150 from the National Cancer Institute and in part by the U. S. Atomic Energy Commission Contract No. AT(04-3)-136, both with the University of Southern California.

† On leave of absence from the University of Southern California, Los Angeles, California.

DISTRIBUTION OF THIS DOCUMENT IS UNLIMITED

Table of Contents

Chapter | Page

1. INTRODUCTORY NOTE 1

2. ATOMIC COLLISION CROSS SECTIONS 2

3. STOPPING POWER FOR HEAVY CHARGED PARTICLES 6

4. RANGE-ENERGY RELATIONS 11

5. SHELL CORRECTIONS AND I-VALUES 14

6. MISCELLANEOUS EFFECTS 16

    A. Charge State Correction 18
    B. Very Low Velocity Particles 19
    C. Small Volumes 22
    D. Channeling 23

7. STRAGGLING OF HEAVY PARTICLES 24

    A. Thin Absorbers 24
    B. Thick Absorbers 26

8. COULOMB AND MULTIPLE SCATTERING, AND NUCLEAR INTERACTIONS 29

    A. Coulomb Scattering 29
    B. Multiple Scattering in Thin Absorbers . . . 30
    C. Multiple Scattering in Thick Absorbers . . . 33
    D. Nuclear Interactions 33

Chapter Page

9. ELECTRONS 34

A. Restricted Stopping Power (LET) 36

B. Practical Considerations for Stopping Power 36

C. Electron Ranges and Energy Deposition in Thick Absorbers 37

10. MEAN ENERGY FOR THE FORMATION OF AN ION PAIR . . . 39

A. Gases 39

B. Solids 39

ACKNOWLEDGMENT 42

REFERENCES 43

TABLES 54

FIGURES 74

1. INTRODUCTORY NOTE

This article presents some of the commonly used formulas and principal data on the passage of fast charged particles through matter. Because of space limitations, much useful material has been omitted. The bibliography includes mainly the newest available references. Most of the technical reports cited are available from the Clearing House for Federal Scientific and Technical Information, Springfield, Va. 22151. An extensive review of the field is found in Publication 1133 of the National Academy of Sciences - National Research Council (NA67). The "Bibliography of Atomic and Molecular Processes" (ORNL-AMPIC 11, UC-34-Physics for January-June 1968), is published semi-annually by the Atomic and Molecular Processes Information Center, Oak Ridge National Laboratory, Oak Ridge, Tennessee. It contains sections concerned with energy losses, ionization, particle range, etc.

A number of papers concerned with particles at the lowest energies considered in this article have appeared in the "Proceedings of an International Conference on Atomic Collisions and Penetration Studies with Energetic Ion Beams", Chalk River, Ontario, September 18-21, 1967 (DA68), and in the abstracts of the "V International Conference of the Physics of Electronic and Atomic Collisions", (FL67).

2. ATOMIC COLLISION CROSS SECTIONS

The following notation will be used:

The kinetic energy of particles will be denoted by T, the energy of a secondary electron (δ-ray) by E or by W if expressed in atomic units [Eq. (2-3)]. Thicknesses s are usually measured in g cm^{-2}. The stopping power (usually called dE/dx) will then be denoted as $S = -dT/ds$.

Except for particles with very small or extremely large velocities v, the interaction between energetic charged particles (of charge ze) and matter leads mainly to the excitation and ionization of atoms or molecules (FA63). The probability for a collision leading to an atomic state of energy E_n is described by the collision cross section σ_n. Relatively little information is available about the details of σ_n (e.g., FC68, RU68, OL67, ES69). In energy loss experiments, the quantities observed are usually averages over E_n and σ_n (e.g., the stopping power dT/ds is $\sum_n E_n \sigma_n$), and even a coarse approximation of σ_n will give satisfactory answers.

Frequently, the free electron approximation is used for a description of σ_n. The energies E_n then are continuously distributed and are equal to the electron energy E. The collision cross section is differential with respect to E and is given, nonrelativistically, by (see, e.g., BI68).

$$d\sigma' = (PZ/\beta^2)E^{-2}\ dE \qquad (2\text{-}1)$$

where $P = 2\pi z^2\ mc^2\ r_o^{\ 2}\ N_o/A = 0.15354 \times z^2/A \quad \text{MeV/cm}^2$

z = charge number of incident particle

β = v/c, velocity of incident particle relative to velocity of light [see Eq. (8-3)]

$r_o^{\ 2} = e^4/m^2c^4 = 7.9408 \times 10^{-26}\ \text{cm}^2$ (square of "classical electron radius")

m = rest mass of electron, $mc^2 = 0.511004$ MeV

N_o = Avogadro's number = 6.02217×10^{23}

e = electron charge

E = energy of electron after collision

A = atomic weight of stopping material, in grams

Z = atomic number of stopping material.

Using the Born approximation, Bethe (BE30) has given the non-relativistic quantum mechanical derivation of $d\sigma$ for bound electrons:

$$d\sigma = 2(P/\beta^2) \sum_i J_i(\eta_i, W)\ dW \qquad (2\text{-}2)$$

where J_i is called the excitation function (WA56).

Electron energies W and equivalent particle energies η_i are measured in atomic units

$$W = E/[(Z - d_i)^2 R_y] \tag{2-3}$$

$$\eta_i = mc^2\beta^2/[2R_y(Z - d_i)^2] = 18,800\ \beta^2/(Z - d_i)^2 \tag{2-4}$$

R_y = Rydberg = 13.60 eV

d_i = electron defect, depending on the atomic shell i

(i = K, L, M, . . . shell)

$d_K = 0.3$

$d_L = 4.15$

The excitation functions J_i have been evaluated, using hydrogenic wavefunctions, for the K, L and M-shells (WA51, WA52, WA56, BI67, KM66, KH68). While J_K probably is reasonably correct for all Z, it appears that J_L is acceptable without modifications for $Z > 30$ only, and J_M will have to be recalculated with more realistic wavefunctions.

An appreciation of the difference between the two approximations, $d\sigma'$ and $d\sigma$, can be obtained from a study of a plot of $J_i\ W^2$ versus W (Fig. 1). Further comments will be made later at appropriate places (see also BI69).

Generally, the Born approximation is valid for $\beta \gg z/137$ (protons with $\beta = 1/137$ have a kinetic energy of 25 keV). Some tests have been made for small particle velocities: for protons incident on helium, the Bethe-Born approximation is valid for energies above 450 keV (TH67), while for the vacuum ultraviolet emission of hydrogen gas, produced by fast protons, it appears to be valid above 150 keV (DD68).

Almost 100 papers concerning atomic and molecular excitation by electron impact alone are listed in the "Bibliography of Atomic and Molecular Processes" for January to June of 1968. In particular, the following may be of interest: ES69, KY68, OL67, VS68.

Measurements of the excitation of the inner shells with protons have been made: KP67, DK68; see KJ68 and ML58 for further references. At low energies it is necessary to take into account the Coulomb deflection of the incident particle to get reasonable agreements with the Born approximation (BL69). Similar corrections are necessary for incident electrons.

3. STOPPING POWER FOR HEAVY CHARGED PARTICLES

Since the stopping power of heavy charged particles depends largely on the velocity and the charge of the particle, but not its mass (IS67), the discussion of this section applies to all heavy charged particles, with the exceptions specified in Sec. 6. The tables and data presented apply to protons and can be converted for other particles with the procedures described in Sec. 6.

The mean energy loss per unit path length is called the stopping power S. It is defined by

$$S = -dT/ds = \int W \, d\sigma = (2P/\beta^2) \sum_i B_i \tag{3-1}$$

where the stopping number B_i is defined by

$$B_i = \int_{I_i}^{\infty} J_i \, W \, dW \tag{3-2}$$

$I_i = W_{min}$ is the energy to lift an electron from the i-th shell to the lowest unoccupied atomic level, and the integral includes a sum over the discrete atomic energy levels. For large velocities, Bethe (LB37) has derived the asymptotic expression

$$B' = \Sigma B'_i = Z \ln(2mv^2/I_{ave}) \tag{3-2a}$$

I_{ave} is defined in Eq. (5-1). B_L and B'_L are shown in Fig. 2. The "shell corrections" are defined by

$$\Sigma C_i (\eta_i, Z) = B' - \Sigma B_i \tag{3-3}$$

and are thus an integral part of the quantum mechanical theory. For higher order Born approximations they will presumably depend on the particle charge z.

If S is calculated using the free electron cross sections $d\sigma'$, an unphysical minimum energy $E_{min} = I_e^2/2\,mv^2$ has to be used as the lower limit of the integral to get approximately the correct stopping power:

$$S' = (P/\beta^2)\int_{E_{min}}^{2mv^2}(Z\ E/E^2)\ dE = (2PZ/\beta^2)\ \ln(2mv^2/I_E) \qquad (3\text{-}4)$$

This choice of E_{min} is necessary to take into account the increase of J over J′ at small energies W (see Fig. 1) but it will not give exact agreement with the quantum mechanical theory. To achieve this, it is necessary to choose

$$I_e = I_{ave}\ \exp\,(\Sigma\ C_i/Z) \qquad (3\text{-}5)$$

where I_e now of course is energy dependent.

For the practical calculation of stopping power, the following, relativistically correct, formula is used:

$$S = -dT/\rho ds = (0.30708/\beta^2)z^2(Z/A)\ [f(\beta) - \ln I_{ave} - \Sigma\ C_i/Z - \delta/2] \qquad (3\text{-}6)$$

Stopping power in units MeV cm^2/g = keV cm^2/mg, and z, β, Z and A are defined with Eq. (2-1).

ρ = density of stopping material

C_i = shell correction of the i-th shell

δ = density correction at high energies

I_{ave} = average excitation potential per electron of stopping atom (including low-velocity density effect), a constant by definition.

$$f(\beta) = \ln [2\, mc^2\beta^2/(1-\beta^2)]-\beta^2 \qquad (3\text{-}7)$$

β^2 and $f(\beta)$ are listed in Table I as functions of the kinetic energy T of several particles. $f(\beta)$ is applicable for any charged particle of velocity $v = \beta c$ and mass $M >> m$. If an ion of mass M_i and kinetic energy T_i is under consideration, its velocity can be found by looking up in Table I the value of β corresponding to a proton energy

$$T = T_i/m_r \qquad (3\text{-}8)$$

where $m_r = M_i c^2/938.259$ MeV.
The shell corrections can be obtained from Fig. 4, and I-values from Fig. 5.

For most metals the density effect δ is negligible for proton energies below 1000 MeV. For details see ST67, FA56 and p. 69 of BK58. Experimental confirmation is found, e.g., in NM67.

At low energies (proton energies of less than 0.5 MeV, alpha particle energies below 2 MeV), the charged particle will not have its full charge (see Sec. 6).

A list of values for S computed (ref. BJ67) from Eq. (3-6) is given in Table II. For emulsion, see BD63 and BA63. For the other materials, the I-values given in Fig. 5 were used. The shell corrections are discussed in Sec. 5. The density effect is not used.

For proton energies of 0.05 to 12 MeV, the experimental stopping powers for many substances are given in Table III. Most of these numbers are read from the graphs of refs. WH58, and the tables of AH67 and AS68. This seems the best way to average the experimental results, but see also MA68, OR68, WM67, JK68. The stopping cross section in $eVcm^2$ per atom can be obtained by multiplying S with the factor $(A/N_o) \times 10^6$ (Avogadro's number N_o, atomic weight A).

For protons in other elements, interpolation for Z by the method of Lindhard and Scharff (LS53) can be used but direct computation from Eq. (3-6) is recommended. (A discussion of experimental results is found in BK67).

The stopping power of compounds is within a few per cent an additive function of the stopping power of the elements which make up the compound (Bragg rule, see, e.g., BI68 or BT68). Precise measurements at 300 MeV (TH52) have shown deviations of about 1 per cent from additivity. At energies between 4 and 30 MeV energy dependent deviations of up to 3% have been observed for Al_2O_3, SiO_2 and Lucite (TS67 and BT68). At small energies, energy loss measurements (SZ65) have also shown deviations from the Bragg rule.

For the approximation with an analytic function, the expression

$$S = C\,T^{\alpha}$$

may be used over limited energy ranges; e.g. for protons with $5 < T < 20$ MeV in Ge, $C = 136.7$ and $\alpha = -0.7313$ will be accurate to better than 0.4% (see BI68 for other values). If particles of initial energy T are absorbed in a material of thickness s, the mean residual energy $\overline{T}_1$ of the particles can be calculated directly:

$$\overline{T}_1 = (C_R\, T^{\gamma} - s)^{1/\gamma}$$

where $C_R = (C\,\gamma)^{-1}$ and $\gamma = 1 - \alpha$.

If the stopping power is used, successive approximations have to be calculated. The computer program of BJ67 produces the coefficients C, C_R and α.

4. RANGE-ENERGY RELATIONS

As long as fewer than about 40% of the particles are removed from the incident beam by nuclear reactions, the median projected range $R_m(T)$ is defined as the thickness of material through which one-half of the incident monoenergetic charged particles of energy T are transmitted (see p. 203 of ref. BI68).

The mean range of monoenergetic particles of kinetic energy T is defined by

$$R(T) = \int f(R)\ R\ dR \tag{4-1}$$

where f(R) is the experimentally measured distribution function (the "probability density" of the mathematicians) and can be determined quite readily in cloud or bubble chambers and in photographic emulsions (except for problems connected with the last bubble or grain). It is not a practical quantity for experiments in which the tracks of the particles cannot be followed. In particular, the mean projected range is difficult to determine experimentally because of the removal of particles from the beam due to nuclear reactions and multiple scattering.

At energies higher than a few MeV, the number of particles is sensibly reduced owing to nuclear reactions (ref. KO64, BI60 and BA61), and appropriate corrections have to be applied (see Sec. 8D).

The quantity related to R(T) which can be calculated from stopping power theory is the theoretical mean range $R_t(T)$ in the continuous slowing down approximation (csda):

$$R_t(T) = \int_{T_1}^{T} S^{-1}\, dT \qquad (4\text{-}2)$$

In principle, T_1 is the thermal energy of the particle. For small velocities the description of the stopping power given in Sec. 6B can be used. If S is not known accurately at these energies, a more accurate result for $R_t(T)$ may be obtained if T_1 is chosen to be a higher energy (e.g., 1 MeV for protons) and an experimental value of $R(T_1)$ is added to the integral to take care of the low energy contribution to the range. For experimental measurements it will be necessary to consider the detector threshold energy as the energy T_1 (BM57 and HP60).

A small difference between R(T) and $R_t(T)$ is caused by the use of the csda approximation (LE52 and TT68). A simple relation exists between the ranges for different particles. It is discussed in Sec. 6.

Mean csda ranges for protons in several elements have been computed (ref. BJ67) by numerical integration of the values of Tables II and III. They are listed in Table IV. Values for R(1 MeV) are obtained from refs. BF60, MR67 and RY55. For other elements, the method of ref. SU60 can be used to obtain range-energy relations. For other particles (mesons or heavier ions) see Sec. 6. Extensive tabulations can be found in refs. JA66, BJ69, BB67 and NO67.

For high energies ($\varepsilon >$ 1,000 MeV for protons) nuclear interactions absorb most of the particles and range becomes a rather meaningless term.

While the straggling in pathlength can be represented approximately by a gaussian (see Sec. 7), the asymmetry of multiple scattering (the zig-zag path taken by a particle can only be longer than the foil thickness, see Sec. 8), and the residual skewness of the electron-loss straggling cause an asymmetry in the range straggling. The median range therefore, is different from the mean range.

The total median range $R_m(T)$ (equal to the foil thickness), neglecting the straggling asymmetries, can be obtained from the computed mean pathlength $R_t(T)$ by the application of the multiple-scattering correction ΔR:

$$R_m(T) = R_t(T) - \Delta R \ .$$

The relative correction of $\Delta R/R$ for several elements is plotted in Fig. 3. Further discussion is given in refs. BU60, BF61, BZ67 and TB68. No discussion of the relation of mean and median range seems to be available (see Sec. 7).

5. SHELL CORRECTIONS AND I-VALUES

In principle, the stopping power S can be calculated theoretically using atomic collision cross sections [Eq. (3-1)]. At present, no complete sets of cross sections for all shells are available, and the expression Eq. (3-6) is used for the calculation of S. The unknown functions B_K, B_L,... are then replaced by one unknown constant, $I=I_{ave}$, and the unknown functions C_i, which are important only at small energies. If extensive experimental data are available, the shell corrections $C/Z = \Sigma C_i/Z$ can be determined experimentally (AN69), together with the I-value. Usually, experimental uncertainties and limited coverage in energy do not permit this approach. In a modification of an earlier approach (BI61), it is suggested now, that, for $8 \leq Z \leq 25$, Walske's shell corrections (WA52, WA56, BI67, KH68) be used in modified form:

$$C/Z = [C_K + V\ C_L(H\ \beta^2)]/Z \qquad (5\text{-}1)$$

with parameters H, V and I determined in a least squares fit to experimental data. Similarly, for $Z \leq 8$, $C/Z = V\ C_K(H\beta^2)$. For $Z \geq 25$, Bonderup's shell corrections C_B (BO67) are used, also in a modified form:

$$C/Z = V\ C_B(H\ v^2/v_o^2 Z)/Z \qquad (5\text{-}2)$$

Good fits to experimental data for protons and deuterons are obtained as long as $C_B \geq 0$. Values for H, V and I may be found in BJ67. Typically, for $Z \geq 47$, $H = 0.755$, $V = 0.68$ and $I_{Ag} = 476$ eV, $I_{Au} = 780$ eV. For $Z = 29$, $H = 0.55$, $V = 0.61$ and $I_{Cu} = 319.5$ eV. These fits include effects due to the higher Born approximations and are therefore only valid for particles of charge +e.

It was found that the least squares fits do not show singular and distinct minima. For experimental data covering a limited energy range, different local minima will give almost the same χ^2. This is fairly obvious from [Eq. (3-6)]: for a limited velocity range, an increase in I can be almost entirely compensated by a decrease in the shell corrections.

Values of C/Z for protons and deuterons adopted in this paper are given in Fig. 4.

While I-values are properly defined by:

$$\ln I_{ave} \equiv \sum_n f_n \ln I_n \qquad (5\text{-}3)$$

(DT68), only a few values for light elements have been calculated with this expression (BE66, WH33). They are not as accurate as the experimental values. The quotient $k = I/Z$ is expected to be a constant if I is evaluated using the Thomas-Fermi model (BL33). Fig. 5 shows a plot of the best available values of k. Both the rise of k for $20 \leq Z \leq 30$ and the oscillation for even and odd values are unexpected. The interpolation schemes suggested in the past (DT68) cannot be considered reliable, and further measurements appear to be very desirable.

6. MISCELLANEOUS EFFECTS

A difference in the ranges of positive and negative mesons has been observed (BD63, HL69). Similarly, Andersen, Simonsen and Sørensen (AS69) found a difference between the stopping power of particles of charge one (p,d) and of charge two (He^3, He^4). This difference presumably is caused by effects due to higher Born approximations. In the further discussions of this section, these effects are implicitly included in the definition of z^*.

The first Born approximation used in the derivation of the collision cross sections, Eq. (2-2), is valid for $\beta >> \beta_1 = z/137$. For particles with $\beta < \beta_1$, atom-atom collisions will contribute increasingly to the stopping process, and an approach based on the use of the Thomas-Fermi model of both the incident ions (with an effective charge $z^*e < ze$) and the absorber atoms has been fruitful (see Sec. 6B).

The stopping power S_M for any particle of mass M, nuclear charge ze (values for different particles are given in Table V) and kinetic energy T can be calculated from the proton stopping power S_p with:

$$S_M(T) = z^{*2} S_p(\tau) \qquad (6\text{-}1)$$

where $\tau = T/m_r$ and z^* is discussed in Sec. 6A. Similarly, a simple relation exists between the range R_M of the particle and the range R_p of a proton:

$$R_M(T) = (m_r/z^2) R_p(\tau) + m_r z^{2/3} C_z(\beta/z) \qquad (6\text{-}2)$$

where $m_r = Mc^2/938.259$ MeV, and the second term is called the range extension caused by the reduced charge z^*. C_z is a universal function for any ion in a specific substance. For emulsion, C_z is found in Fig. 5 of ref. HP60 and it is defined for any substance in Eq. (7) of ref. HP60 (see BB67 for data). Another approach can be used: Use Eq. (6-2) to find the range difference $R_M(T) - R_M(T_1)$ and add $R_M(T_1)$ as defined in Sec. 6B to find R(T).

In general, a numerical calculation for a specific case, using Eq. (3-6) with appropriate effective charge z^* will be preferable to the use of Eq. (6-2).

Examples

1. The mean range of 20 MeV muons ($m_r = 0.1126$ from Table V) in Aℓ is:

$$R_\mu(20\text{ MeV}) = 0.1126\times R_p(177.6\text{ MeV}) = 0.1126\times 27.15 = 3.057\text{ gcm}^{-2}$$

2. The mean range of 50 MeV alphas ($m_r = 3.9726$) in copper is:

$$R_\alpha(50\text{ MeV}) = (3.9726/4)\times R_p(12.602\text{ MeV}) = 0.3219\text{ gcm}^{-2}$$

where R_p is obtained from Table IV and C_z has been neglected. An extensive discussion for heavy ions is given in NO67, with many graphs for different incident particles.

6A. Charge State Correction

For velocities $\beta < \beta_2 = 0.04\ z^{2/3}$ it is observed that the nuclear charge ze is not fully effective. A reduced effective charge z*e is used in Eq. (3-6) instead of the nuclear charge ze (RO60, NO67, HP60). If z* is defined to give the correct observed stopping power, it is not equal to the mean charge per particle of a beam leaving an absorber (PB68, BG65). With an accuracy of about 5%, z* can be obtained from

$$z^*/z = 1 - \exp(-1.316x + 0.1112x^2 - 0.0650x^3) \qquad (6\text{-}3)$$

where $x = 100\ \beta/z^{2/3}$. This expression is valid for $x > 0.27$. In gases, the values are several percent smaller (RS60). It should be noted that the approach described in the next section overlaps the range of validity of Eq. (6-3).

For ions with $21 \leq z \leq 39$, Hvelplund and Fastrup (HV68) have found a periodic dependence of the stopping cross section on z for a carbon absorber. Similar effects were found in WI68 and HA68. Fractional charges for carbon absorbers in CC67 agree with Eq. (6-3) to better than 5% for most ions. The fluctuations for different absorbers found in their Table III could be due to shell corrections.

When available, experimental data should be used. Recent papers include:

Br and I ions in Be, C, Al, Ag, Au	MB66
O^{16} ions in Ag, Au; S^{32} ions in Au	AH68
S^{32}, Cl^{35}, Br^{79}, I^{127} ions in Mylar	PB68
O and Cl ions in C, Al, Ni, Ag, Au	BG65
I^{127} ions in C, Al, Ni, Ag, Au, UF_4	BN67

C, N. O, F, Ne in Be, C	CB68
$21 \leq z \leq 39$ in C	HV68

Interesting results for charge state populations (I^{127} in gas and solid) have been found by Moak et al. (ML68). Many references to earlier work are included.

6B. Very Low Velocity Particles

At low velocities, $\beta \leq \beta_1 = z^{2/3}/137$, ions will carry a reduced charge, and for $\beta \ll \beta_o = 1/137 = 0.0073$, they will be neutral. The collisions then will be between neutral atoms, and are commonly called "nuclear collisions" (LS63, OH63). Even for this case, energy loss to atomic electrons is still possible (LS63). From a Thomas-Fermi description of the atoms, it is expected that the following dimensionless parameters should result in universal range-energy curves:

$$\text{Energy} \quad \varepsilon = 32.53 \times T(\text{keV})\, M_2/[zZ(M_1 + M_2)\sqrt{\zeta}\,] \qquad (6\text{-}4)$$

$$\text{Range} \quad \rho = 1.660 \times 10^5 \times R(\text{mgcm}^{-2})\, M_1/[(M_1 + M_2)^2\zeta] \qquad (6\text{-}5)$$

where

M_1 = Atomic mass of incident particle

M_2 = Atomic mass of absorber material

z = Atomic number of incident particle (usually called Z_1)

Z = Atomic number of absorber material (usually called Z_2)

$\zeta = z^{2/3} + Z^{2/3}$

It is found that the stopping power consists of contributions by electronic and nuclear stopping:

$$S = S_e + S_n. \tag{6-6}$$

From (LS63):

$$S_e = k\sqrt{\varepsilon} \tag{6-7}$$

where

$$k = 0.0793 \times \xi_e\sqrt{zZ}\,(M_1 + M_2)^{3/2}/[(z^{2/3} + Z^{2/3})^{3/4}M_1^{3/2}M_2^{1/2}] \tag{6-8}$$

and ξ_e is approximately given by $z^{1/6}$. This formula is valid for $\varepsilon < 1000$.

The nuclear collision stopping power depends on the ion-atom potential (discussed e.g., in NV66, KE68, LS63, LN68). From Table I of SC66, the following analytic form has been derived (similar to an expression given in BS68)

$$\left(\frac{d\varepsilon}{d\rho}\right)_n = 0.5455\ \ln(\varepsilon)/[\varepsilon(1-0.9988 \times \varepsilon^{-1.5391})] \tag{6-9}$$

and

$$S_n = 1.96 \times 10^{-4}\ \frac{d\varepsilon}{d\rho}\, M_2(M_1 + M_2)\sqrt{\zeta}/(zZM_1) \tag{6-10}$$

S_n in keV/mg cm^{-2}.

It is seen that $(d\varepsilon/d\rho)_n$ is a universal function of ε, while S_e, through k, depends on zZ. It is therefore only possible to produce a universal range curve $\rho(\varepsilon) = \int_0^{\varepsilon} d\varepsilon'/(d\varepsilon'/d\rho)_n$ for the nuclear collisions, and if the electronic collisions are of importance, different range curves will be obtained for different values of k.

Different quantities have been defined to describe the path taken by the particle: Linear Range (total path-length), Vector Range (vector distance from point of incidence to stopping point), and Projected Range (projection of vector range onto direction of incidence). A particle will experience only few collisions, e.g., for $T = 12$ keV argon atoms in a germanium absorber, the mean collision number is ~ 6 (KE68). Both statistical and continuous methods have been used to calculate mean ranges.

For $M_1 \geq M_2$, the ratio of mean projected range $\overline{R_p}$ and linear range R is approximately $R/\overline{R_p} \sim 1 + M_2/3M_1$ (LS63, MS65). A modification of this procedure is suggested in MS65, giving a better agreement with experiment for $\varepsilon < 1$.

Using Eqs. (4-2) and (6-10), range-energy curves have been calculated (SC66) for different values of k, and are plotted in Fig. 6. In general, the agreement between theory and experiment is satisfactory, with accuracies of about 20%: AG68, BL68, BS68, CA68, JD67, LS67. The use of logarithmic scales in the plots of experimental data tends to hide the differences. Usually, the value of k in Eq. (6-7) is considered an adjustable parameter, and better agreement with the theory can then be achieved (e.g., CS68, CB68).

Moak and Brown (MB66) and Kahn and Forgue (KF67) have found deviations from the $\sqrt{\varepsilon}$ behavior predicted by

Eq. (6-7) for $\varepsilon \sim 200$. The deviations in k for light elements are not unexpected: the Thomas-Fermi model may not give a good approximation for $Z < 20$.

At higher values of ε (say $\varepsilon > 300$), the approach presented here overlaps with the Bethe theory using effective charges (Sec. 6A) and experimental data have to be consulted to find the more reliable approach.

6C. Small Volumes

The energy losses discussed in Sec. 3 are as experienced by the charged particles and are not directly related to the energy gained by the absorber material (see the discussion of LET in Sec. 9).

Examples

a) In a thin silicon detector of the transmission type, in a vacuum, some δ-rays will leave the back surface of the detector, reducing the observed energy loss slightly (for 40 MeV protons in a 200 μm detector, the reduction amounts to no more than 0.5%).

b) In very small volumes (diameter of 1 μm or less of a material of density $\rho = 1\ \mathrm{g/cm^2}$, corresponding to the size of living cells), the energy lost by a particle of moderate or large energy is quite uncorrelated to the energy absorbed in the volume. Since the behavior of low energy electrons is not well known (energies of less than 1 keV), and since the collision cross sections are not known for low Z materials, calculations are extremely unreliable at present.

6D. Channeling

In single crystals it is observed that energy loss depends on the direction of the particle path with respect to the crystal axes. A detailed discussion of various aspects of the problem is given by Lindhard (LI65). Other calculations are available in several of the experimental papers mentioned below and in BR68.

If particles travel parallel to a major axis of the lattice, some can move "in between" the atoms, reducing the number of collisions with small impact parameters (energy loss and straggling would then both be reduced, see AE67, DM69) while others would move close to nuclear positions, increasing the effects. For a well collimated beam with small multiple scattering, a fraction of the beam may keep away from atoms for long distances.

A number of experiments have recently been published: an especially instructive diagram is given in RS67, a study of 3-11 MeV protons in Si and Ge is of interest for the use of solid state detectors: AE67. Other studies are described in DW68, DM69, ER67, RO69, SV68.

7. STRAGGLING OF HEAVY PARTICLES

Particles, in passing through an absorber of thickness s, experience a random number of collisions with a wide range of possible energy transfers. The energy losses Δ of a monoenergetic beam of particles thus will fluctuate ("Straggling") about the mean energy loss $\bar{\Delta} = s S$. The straggling distribution function $f(\Delta)$ depends on the velocity $v = \beta c$ of the incident particle, on S and Z/A of the material. For large thicknesses, $f(\Delta)$ approaches a gaussian shape.

7A. Thin Absorbers

Landau (LA44), Symon (SY48), Vavilov (VA57), Shulek, *et. al*. (SG67) and many others have discussed straggling in thin absorbers. Extensive tabulations are available for the Vavilov distribution (SB67), based on calculations using the free electron collision spectrum [Eq. (2-1)].

A comparison of experimental data (e.g., KO68, MR68, AL69) with the theory can be based on the use of the *moments* of the distribution function. The central moments C_n are defined by:

$$C_n = \int f(\Delta)\ (\Delta-\bar{\Delta})^n\ d\Delta = \langle(\Delta-\bar{\Delta})^n\rangle \qquad n = 0,1,2,3,\ldots \qquad (7\text{-}1)$$

and $f(\Delta)$ must be normalized, i.e.

$$C_o = \int f(\Delta)\ d\Delta = 1. \qquad \text{Obviously } C_1 = 0.$$

The theoretical quantities κ_n (the "cumulants" of statistical theory, FA53) related to these moments, calculated with the Vavilov approach, are given by (s in gr cm^{-2})

$$\kappa'_n = \frac{0.1535\ Zz^2}{\beta^2\ A}\ \frac{s\ E_{max}^{n-1}}{n-1}\ [1-\beta^2(n-1)/n]\ (\mathrm{MeV})^n \qquad (7\text{-}2)$$

where $E_{max} \simeq 2\ mc^2\ \beta^2/(1-\beta^2) = 1.022\ \beta^2/(1-\beta^2)$ (7-3)

In particular (e.g., BO48):

$$\kappa'_2 = \frac{0.1569\ Zz^2}{A}\ s\ (1-\beta^2/2)/(1-\beta^2)\ \mathrm{MeV}^2 \qquad (744)$$

For $n = 2, 3$ $\quad C_n = \kappa_n$

$n = 4$ $\quad C_4 = \kappa_4 + 3\ C_2^2$ $\quad$ etc.

The standard deviation $\sigma = \sqrt{\kappa'_2}$ of a straggling distribution thus is quite insensitive to the incident particle energy. Except for a gaussian, there is no simple relation between the "width at half maximum" and σ. For practical applications, it will be best to calculate moments by numerical integration from experimental data, and compare them with κ_n. For the actual functions, ref. SB67 should be consulted. For applications in thin silicon detectors, see Fig. 7.

The Vavilov function will be an approximation due to the use of the free electron collision cross section. No complete quantum mechanical calculations are available. An estimate of the deviations to be expected can be obtained from a comparison of moments $M_n = \int W^n J\ dW$ using J_K and J_L. Some of these ratios are given for J_L in Figs. 8 and 9 (BI69). For example, for protons in silicon, the maximum deviation in M_2 is expected to occur at $\eta_L = 1.6$, corresponding to a kinetic energy $T \sim 3.5$ MeV. The correction by Shulek et al. (SG67) takes into account only M_2 and therefore cannot be expected to be reliable. It is also much too large for small velocities. Experiments by Nielsen for several elements (NI61, Fig. 7) indicate deviations of the second moment amounting to no more than 20% from $\kappa_2' = s\,M_2'$ while Shulek et al. indicate deviations of up to 100%.

7B. Thick Absorbers

An extensive discussion for large energy losses is given by Symon (SY48) and by Tschalär (TS67, TS68, TT68). For moderate energy losses, Tschalär's results for heavy particles of initial kinetic energy T and residual mean energy T_1 can be approximated by the following expression for the second moment (accurate to about 2%).

$$C_2 = \kappa_2' Q$$

where $Q = (T/T_1)^{1/3}$	for	$B/Z \sim 2.3$	and	$T_1/T > 0.4$
$= 0.99\ (T/T_1)^{1/2}$		$B/Z \sim 3.5$		$T_1/T > 0.4$
$= 0.985\ (T/T_1)^{2/3}$		$B/Z \sim 6.9$		$T_1/T > 0.6$

where B is the stopping number, Eq. (3-3), and

$$B/Z = f(\beta) - \ln I - \Sigma C_i/Z$$

For larger energy losses, TS68 should be consulted. For the asymmetry of the curves, the third moment should be studied. Tschalär uses the skewness parameter $\gamma_3' = C_3/C_2^{3/2}$ for this purpose. From his results it is found, that the expression for thin absorbers: $\gamma_3' = \kappa_3'/(\kappa_2')^{3/2}$ is accurate to a few percent for $B/Z \sim 2.3$ and $T_1/T > 0.5$ and for $B/Z \sim 6$ and $T_1/T > 0.7$. It may be noted that the distribution functions for the cases discussed above are approximately given by the Vavilov functions for the value $\kappa_v = 0.25\ \gamma_3^{-2}$ of the Vavilov parameter $\kappa_v = \xi/E_{max}$ (SB67).

For the ranges R of particles with a mean value $\overline{R}$ the second central moment, also called the "mean square fluctuation" σ^2 is defined by

$$\sigma^2 = \langle R^2 \rangle - \overline{R}^2 \tag{7-5}$$

The distribution f(R) is usually approximated by a gaussian:

$$f(R) \approx \frac{1}{\sigma\sqrt{2\pi}} \exp\left[-(R-\overline{R})^2/2\sigma^2\right] \tag{7-6}$$

and the probability p of finding a particle with range between R and R + dR is pdR = f(R)dR. The deviations from a gaussian are small, but not negligible. They are discussed in LE52 and TT68. Their influence on the Bragg curve has not been studied yet.

The ratio of σ to the total mean range R is given in Fig. 10 for protons in several elements. For other particles of mass M, the value can be calculated from:

$$\left(\frac{\sigma}{R}\right)_M = \sqrt{1/m_r}\left[\frac{\sigma}{R}\,(T/m_r)\right]_{\text{proton}} \qquad (7\text{-}7)$$

Estimates for the quantum mechanical corrections have been incorporated in the calculations for Fig. 10. The values of $\frac{\sigma}{R}$ are considerably smaller than the values calculated by Sternheimer (ST60), but they are still slightly larger than experimental values (BU60), which were evaluated neglecting the skewness of the range straggling curves. The observed straggling in range-energy measurements is composed of the energy loss straggling, and an additional asymmetric contribution caused by the multiple scattering process (BU60, BI60).

8. COULOMB AND MULTIPLE SCATTERING, AND NUCLEAR INTERACTIONS

8A. Coulomb Scattering

The differential cross section for Coulomb scattering of a charged particle of kinetic energy T (in MeV), momentum p, velocity v and charge ze by a nucleus of charge Ze and mass number A into the solid angle $2\pi \sin\theta \, d\theta$ is given by the Rutherford formula:

$$d\Phi(\theta) = \frac{2\pi e^4 z^2 Z(Z+1)}{4p^2 \, v^2 \, \sin^4(\theta/2)} \; \sin\theta \, d\theta$$

$$\cong \frac{0.814 \; z^2 Z(Z+1)}{T^2} \; \frac{\sin\theta \, d\theta}{\sin^4(\theta/2)} \times 10^{-26} \; \mathrm{cm}^2 \qquad (8\text{-}1)$$

where θ is the angle of scattering from the incident direction. The above formula assumes that the mass of the incident particle is negligible compared with the mass of the nucleus.

Deviations from the Rutherford formula will occur at large angles as the particles begin to feel the influence of nuclear forces. An estimate of the minimum energy T_m for which a deviation can be expected at $\theta = 180°$ can be obtained from

$$T = z \; Z/(\sqrt[3]{A} + 3) \; \mathrm{MeV}$$

A detailed discussion is found in EP61 and JA68. At small angles, the cross section will be smaller than given by Eq. (8-1) because the atomic electrons will shield the nuclear charge. The Rutherford cross section is reduced by 10% at an angle θ_q given by (from MO47):

$$\theta_q = \theta_o \sqrt{61.7 + 421\ \alpha^2} \quad \text{and by 50\% at}$$

$$\theta_r = \theta_o \sqrt{2.75 + 10.85\ \alpha^2}$$

where $\theta_o = \dfrac{0.244 \sqrt[3]{Z}}{pc\ (\mathrm{MeV})} \sim \dfrac{0.244 \sqrt[3]{Z}}{\sqrt{2M_oc^2\ T}}$

and $\alpha = \dfrac{Z\ z}{137\beta}$. For large kinetic energies,

$pc = \sqrt{T^2 + 2TM_oc^2}$, and with $\zeta = T/M_oc^2$,

$$\beta^2 = \zeta\ (\zeta + 2)/\ (\zeta + 1)^2 \tag{8-3}$$

Example: 10 MeV alpha particles in Au: from Table I, $\beta = 0.073$, $\alpha = 15.8$. $\theta_o = 1.05/\sqrt{74{,}600} = 3.84 \times 10^{-3}$ degrees. Finally, $\theta_q = 3.84 \times 10^{-3} \sqrt{61.7 + 105{,}000} = 1.25°$. This reduction is of great importance in the derivation of the multiple scattering formulas.

8B. Multiple Scattering in Thin Absorbers

Multiple Coulomb scattering in thin foils will cause a parallel beam of particles to spread out into a cone. Recent discussions are found in HF68, SC63 and GD68.

Moliere's theory (MO48, BE53 and MO55) is a small-angle approximation to the general problem (BR59, NS61 and TM59) which is in agreement with experimental results, with the possible exception of electrons in heavy elements and also possibly at small energies ($\beta^2 < 2 \times 10^{-3}$).

The characteristic quantity occurring in the theory is the angle θ_o, defined by $\theta_o = \theta_1 \sqrt{B}$ where

$$\theta_1{}^2 = 0.157 \frac{Z(Z + 1)z^2}{A} \quad \frac{s}{(pv)^2} \tag{8-4}$$

θ_1 is in radians; s is the foil thickness in g cm^{-2} , p the momentum, and v the velocity of the particle (pv in MeV); z, Z and A have the same meaning as in Sec. 2. B is defined in ref. MO48; for practical purposes it can be obtained from ref. MZ67 or from Table VI for particles with charge 1 with an accuracy of better than 5 per cent. A few values are listed for $z > 1$. It is not obvious whether z^* or z should be used for a computation of the multiple scattering of heavy ions. The use of z^* is suggested. For $z \geq 6$ and $Z \geq 50$, all values $B(\beta,z)$ are larger than $0.98 \times B(\beta=0,\ z=1)$, and for $z \geq 6$ and $Z \geq 20$, all values $B(\beta,z) \geq 0.95 \times B(\beta=0,\ z=1)$.

Moliere's theory modified by Nigam et al. (NS61) gives the distribution function F(x)dx for the relative number of particles entering a cone of angle x and width dx . The reduced angle x is defined by

$$x = \theta/\theta_o$$

An extensive discussion of the problem is given in (MZ67). Table VII giving F(x) is obtained from (MZ67).

Also of interest is the relative number N/N_o of particles entering a cone of half angle α:

$$\frac{N}{N_o} = \int_0^{\alpha/\theta_o} f(x)\ x\ dx \qquad (8\text{-}5)$$

Values are given in Table VIII. For experimental tests of the theory, see BI58, MO58, LO67, BN66.

Example

2-MeV protons penetrating 3 mg cm^{-2} of Ni foil. The average energy in the foil is 1.87 MeV. $\beta^2 \sim 3.96 \times 10^{-3}$ from Table I, $B \sim 7.7$ from Table VI. $\theta_1{}^2 = 4.72 \times 10^{-4}$, $\theta_o = 6.03 \times 10^{-2}$ rad = 3.46 deg. Thus, inside a cone of half angle 7 deg, all but about 6.3% of the protons will be found (see Table VIII).

Caution has to be used for the case of the incident particle of mass approximately equal to or larger than the mass of the scattering nucleus. In this case a considerable fraction of the energy can be lost to the recoil nucleus. This effect is, of course, not included in the fundamental energy-loss formula, Eq. (3-6).

8C. Multiple Scattering in Thick Absorbers

For thick absorbers, the mean energy correction due to multiple scattering has been calculated in TB68 for energy losses between 0.5 T and 0.1 T, for $10 < T < 140$ MeV, for detector angles between 0.005 rad and 0.5 rad for protons in Al, Ag, and Au.

The multiple scattering correction for median ranges has been discussed in Section 3.

8D. Nuclear Interactions

Heavy charged particles will be removed from beams by nuclear interactions: the beam intensity will be attenuated exponentially

$$I = I_o \, e^{-s\Sigma} \tag{8-6}$$

where I is the flux density, and Σ is the macroscopic cross section $\Sigma = \sigma_t \, n$ (σ_t total microscopic cross section, n = number of nuclei per cm^3). For estimates, $\Sigma = 0.32/A^{1/3}$ cm^2/gm may be used (A = atomic number of absorber).

9. ELECTRONS

While electrons in passing through matter will experience interactions similar to heavy-particle interactions, two basic differences are manifest:

a) In the collisions with atomic electrons, large energy losses can occur; and

b) Electrons with energies of only a few hundred kiloelectron volts will show relativistic effects.

An extensive review of the theory is found in (BI58), and extensive tabulations are contained in (BS67). The derivation of the stopping power formula is similar to the heavy particle case. It will be assumed that after a collision by a negative electron, the electron with the higher velocity will be considered the primary. The mean collision loss in MeV cm^2/g is given by (BS67):

$$-\left(\frac{dT}{\rho ds}\right)^{\pm}_{col} = \left(\frac{0.1535}{\beta^2}\right)\left(\frac{Z}{A}\right)\left[\ln\left\{\frac{2(\tau + 2)}{(I/mc^2)^2}\right\} + F^{\pm}(\tau,\Delta) - \delta\right] \tag{9-1}$$

where for electrons $\Delta = 1/2\ \tau$ and

$$F^{-} = -1 - \beta^2 + \ln[(\tau - \Delta)\Delta] + [\tau/(\tau - \Delta)] + \frac{\frac{1}{2}\Delta^2 + (2\tau + 1)\ln[1 - (\Delta/\tau)]}{(\tau + 1)^2} \tag{9-2}$$

and for positrons $\Delta = \tau$ and

$$F^{+} = \ln(\tau\Delta) - \frac{\beta}{\tau}\left[\tau + \Delta - \frac{(5/4)\Delta^2}{(\tau + 2)} + \frac{(\tau + 1)(\tau + 3)\ \Delta - (1/3)\Delta^3}{(\tau + 2)^2} - \frac{(\tau + 1)(\tau + 3)(1/4)\Delta^4 - (\tau/3)\Delta^3 + (1/4)\Delta^4}{(\tau + 2)^3}\right] \tag{9-3}$$

Here $\tau = (T/mc^2)$, δ is the density correction, and $mc^2 = 511004$ eV, Δ is the maximum energy given to δ rays, divided by mc^2. The other symbols here have the same meaning as in Eq. (3-6). In particular, the same I-values are used as for the heavier particles.

The shell corrections are not included, because their contribution above 0.1 MeV amounts to less than 1 per cent. If desired, the shell corrections discussed above (Fig. 4) can be used to correct stopping power values obtained from Eq. (9-1). The differences between electrons and positrons have been studied by Rohrlich and Carlson (RC54).

The energy loss due to bremsstrahlung is important for electrons at relatively small energies. An estimate of the ratio r of the bremsstrahlung energy loss to $(dT/ds)_{coll}$ is given by

$$r \sim T(Z + 1.2)/700 \qquad (T \text{ in MeV}) \qquad (9\text{-}4)$$

at $T_c \sim 700/(Z + 1.2)$ MeV the two energy losses are equal. An important quantity is associated with the traversal of matter by electrons of energies above T_c; this is the distance X_o in which an electron's energy is reduced to $1/e = 0.3679$ of its original value. X_o is called the "radiation length" and is given in Table IX together with more accurate values of T_c. Recent experimental results are found in DR68.

9A. Restricted Stopping Power (LET)

Secondary radiation (δ-rays or bremsstrahlung photons) may travel quite far from the track of a particle. An estimate of the energy deposited inside of a small cylinder around a track can be obtained by setting the quantity Δ in Eq. (9-1) equal to the energy of δ-rays capable of escaping from the volume of interest. Heavy particles produce relatively few δ-rays of high energy (see Eq. 2-1) and the difference between LET and dT/ds is relatively small for energies below Mc^2 (see Sec. 6C, though).

9B. Practical Considerations for Stopping Power

Computed values of the electron stopping power are given for some elements in Fig. 11. Extensive tables are found in (BS67). For $T < 5$ MeV, $(dT/\rho\ ds)_{coll} \sim Z^{-1/4}$. This factor should be used for interpolation in Fig. 11.

Straggling (discussed in detail in KM61) is much larger for electrons than for heavier particles (see, e.g., Fig. 12 in BI68 or Fig. 2 in BR64). The width at half maximum of a straggling distribution may amount to more than 50% of the mean energy loss. Multiple (VV68) and back scattering contribute to the problem. Comparison of mean energy losses calculated from Eq. (9-1) with experimental data (e.g., HU57, HA59, HR68) can be expected to be accurate to better than 10% only if a detailed study of straggling etc., has been made. A comparison of experiment and theory for 1 and 2 MeV electrons in silicon is found in SI67.

9C. Electron Ranges and Energy Deposition in Thick Absorbers

For electrons traversing thick absorbers, lateral and backscattering will be very important and electron distribution functions will extend over wide ranges in space, angle and energy. A general treatment is found in BE63, KK68, RO68, SP55 and SP54. Practical results for many substances are given in SP59, KE66, BS67, LP57 and PE62 and KK68. Detailed investigations have been performed for 5 to 30 keV electrons (CT65), and for 40 to 160 keV electrons (GF59). For higher energies, see, e.g., BH58. Electron ranges calculated by the use of Eq. (4-2) do not have a simple relation to any observed quantity: see Table X.

The practical range-energy relation for electrons is not strongly dependent on the atomic number of the stopping material. Only that for aluminum is given. Monoenergetic electrons are absorbed as indicated in Fig. 12 which serves to define the "practical range" R_p and the "maximum range" R_o. The practical range, in aluminum is given by

$$R_p = 0.537\ T\ [1 - 0.9815/(1 + 0.003123\ T)] \qquad (9\text{-}5)$$

R_p in mg cm^{-2}, T in keV, for the energy range 0.3 keV $\leq T \leq$ 20 MeV, with an accuracy of about ± 6% (KK68). A graph of this relation is given in Fig. 13.

The formulas given above for monoenergetic electrons can be used for continuous beta-ray spectra where R_p and T_o refer to the maximum beta-ray range and energy, respectively. For a discussion of the methods of determining the range from an absorption curve, see KP52.

For practical applications in which information on electron range and energy deposition is required, it appears best to use Spencer's calculations (SP59, see also BI68), but some information is found also in KK68.

Unlike the case for heavy charged particles, determination of electron energies from transmission measurements is not accurate enough for most applications. Energies can be determined much more accurately by measurements with calibrated scintillation or solid state detectors.

10. MEAN ENERGY FOR THE FORMATION OF AN ION PAIR

10A. Gases

The energy loss w of a charged particle per ion pair formed in the material traversed is nearly independent of the energy and type of particle for velocities $\beta^2 > 10^{-4}$ z as can be seen in Table XI. For further values see MY68.

From the measurements of Phipps, Boring and Lowry (PB64), the following approximate velocity dependence of w has been derived for ions with $A < 40$

$$w = 0.119/\beta \quad \text{(eV)} \qquad \text{for } \beta \leq 0.0043$$

For more accurate values, PB64, BS65 and LH65 should be consulted. For ^{206}Pb ions with T = 103 keV, measurements have been made by Cano (CA68).

Mixtures of gases do not follow a simple additivity rule for the value of w (MY68, BH54). A large drop in w of argon for small concentrations of C_2H_4 has been observed. For further details, see MY68. Ionization fluctuations and the resolution of ionization chambers is discussed extensively in AK67.

10B. Solids

A recent discussion of the response of NaI(Tl) to heavy ions is found in KA68, with references to earlier work.

The ionization in silicon and germanium has been studied extensively (see almost any issue of "IEEE Transactions on Nuclear Science"). The average energy ε for the generation of an electron-hole pair is much smaller than for gases. For Si, $\varepsilon \sim 3.6$ eV, for Ge, $\varepsilon \sim 2.96$ eV. For silicon, the following effects have been observed:

a) For low energy electrons (produced with γ-rays), pulseheights, after correction for charge collection efficiency, are proportional to energy within 0.2% (ZM69).

b) For a change in temperature from 300 K to 90 K, an increase of 4% in ε has been observed (PG68).

c) ε is about one percent smaller for alpha particles than for electrons (PG68).

d) For heavy ions, ε is energy dependent at small energies (BB63, FK67, FS69, KA67, RB69, SA65). For $T_m >> 6$ M (keV) (M = atomic mass of ion), the energy T_m' calculated from a measured ionization pulse should be increased by an amount $\Delta T \sim 4$ M (keV), the "ionization defect".

The ionization defect (FS69) is for:

protons	1-2 keV
alpha particles	8-12 keV

Somewhat different results have been given in RB69. Similar results have been obtained for germanium detectors (DB67, PR69). Several factors determine the resolution of solid state detectors (BL67, AN67, TS67); some of the more important:

a) Electronic noise and drift of amplifier system

b) Ballistic deficit

c) Pulse pile up

d) Recombination and trapping

e) Channeling (see Sec. 7).

f) Absorption in surface layers

g) Statistics of the number N of electron-hole pairs produced.

Fano (FA47) has shown that the standard deviation of the mean number $\overline{N}$ is: $\Delta N^2 = \langle (N-\overline{N})^2 \rangle = F\,\overline{N}$ where $F \leq 1$. Bilger (BL67) found $F = 0.13$ for germanium. Alkazov et al. (AK67) obtained $F \sim 0.1$ for silicon. The problem is also discussed in DF67.

Energy loss tables for p,d, t, He^3, He^4 and Li^6 with data useful for particle identifier systems are given in BT67 and SK67. Information about the straggling in thin silicon detectors is given in Fig. 7.

Acknowledgment

I am grateful for the hospitality of the Lawrence Radiation Laboratory in Berkeley, where most of the calculations of this paper were performed on the CDC-6600.

References

NOTE: The symbol in the second column indicates the section in which the reference appears.

AE67	6D	B. R. Appleton, C. Erginsoy and W. M. Gibson, Phys. Rev. 161, 330 (1967).
AG68	6B	M. Ait-Salem, H. Gerhardt, F. Gönnenwein, H. Hipp, and H. Paap, Nucl. Inst. Meth. 60, 45 (1968).
AH67	3	H. H. Andersen, C. C. Hanke, H. Sørensen and P. Vajda, Phys. Rev. 153, 338 (1967).
AH68	6A	B. H. Armitage and B. W. Hooton, Nucl. Inst. Meth. 58, 29 (1968).
AK67	10	G. D. Alkhazov, A. P. Komar and A. A. Vorob'ev, Nucl. Inst. Meth. 48, 1 (1967).
AL69	7	D. W. Aitken, W. L. Lakin, and H. R. Zulliger, Phys. Rev. 179, 393 (1969).
AN67	10	G. Andersson-Lindstroem, Nucl. Inst. Meth. 56, 309 (1967).
AN69	5	H. H. Andersen, H. Sørensen, and P. Vajda, Phys. Rev. 180, 373 (1969).
AS68	3	H. H. Andersen, C. C. Hanke, H. Simonsen, H. Sørensen, and P. Vajda, Phys. Rev. 175, 389 (1968).
AS69	6	H. H. Andersen, H. Simonsen and H. Sørensen, Nucl. Phys. A125, 171 (1969).

****

BA61	4	W. H. Barkas, Phys. Rev. 124, 897 (1961).
BA63	3	W. H. Barkas, "Nuclear Research Emulsions", Academic Press (1963).
BB63	10	H. Bilger, E. Baldinger and W. Czaja, Helv. Phys. Acta 36, 405 (1963).
BB67	4,6	W. H. Barkas and M. J. Berger, Paper 7 of NA67.
BB69	6	N. Barash-Schmidt, A. Barbaro-Galtieri, L. R. Price, A. H. Rosenfeld, P. Söding, C. G. Wohl, M. Roos and G. Conforto, Rev. Mod. Phys. 41, 109 (1969).
BD63	3,6	W. H. Barkas, J. N. Dyer and H. H. Heckman, Phys. Rev. Lett. 11, 26 (1963).
BE30	2	H. Bethe, Ann. Phys. 5, 325 (1930).

BE53	8	H. Bethe, Phys. Rev. 89, 1256 (1953).
BE63	9	M. J. Berger in "Methods in Computational Physics," ed. Alder, Fernbach and Rotenberg (Academic Press Inc., New York, 1963), Vol. 1, p. 135.
BE66	5	R. J. Bell and A. Dalgarno, Proc. Phys. Soc. 89, 55 (1966) and 86, 375 (1965).
BF60	4	H. Bichsel and B. J. Farmer, Bull. Am. Phys. Soc. 5, 263 (1960).
BF61	4	W. H. Barkas and S. von Friesen, Nuovo Cim (10) 19, Suppl. 1, p. 41 (1961).
BG65	6,6A	W. Booth and I. S. Grant, Nucl. Phys. 63, 481 (1965).
BH54	10	T. E. Bortner and G. S. Hurst, Phys. Rev. 93, 1236 (1954).
BH58	9	H. Breuer, D. Harder and W. Pohlit, Z. Naturforsch. 13a, 567 (1958).
BH69	5	H. Bichsel, C. C. Hanke and J. Buechner, USC-136-148 (March, 1969).
BI58	8	H. Bichsel, Phys. Rev. 112, 182 (1958).
BI60	4,7	H. Bichsel, Phys. Rev. 120, 1012 (1960).
BI61	5	H. Bichsel, Technical Report, No. 3, University of Southern California.
BI67	2,5	H. Bichsel, USC-136-120 (April, 1967).
BI68	2,3,4,9	H. Bichsel, "Radiation Dosimetry", Ch. 4, Vol. 1, F. H. Attix and Wm. R. Roesch, eds. Academic Press, New York, January 1968.
BI69	2,7	H. Bichsel, USC-136-147 (January, 1969).
BJ67	3,4,5	H. Bichsel, Univ. of California, L.R.L. Technical Report UCRL-17538.
BJ69	4	H. Bichsel, Range Energy Tables (to be published).
BK58	3,9	R. D. Birkhoff, Encyclopedia of Physics, Vol. 34, 34 (Springer, Berlin, 1958).
BK67	3	H. Bichsel, Paper 2 in NA67.
BL33	5	F. Bloch, Z. Phys. 81, 363 (1933).
BL67	10	H. R. Bilger, Phys. Rev. 163, 238 (1967).

BL68	6B	W. W. Bowman, F. M. Lanzafame, C. K. Kline, Yu-Wen Yu and M. Blann, Phys. Rev. 165, 485 (1968).
BL69	2	W. Brandt and R. Laubert, Phys. Rev. 178, 225 (1969).
BM57	4	H. Bichsel, R. F. Mozley and W. Aron, Phys. Rev. 105, 1788 (1957).
BN66	8	A. A. Bednyakov, V. S. Nikolaev, A. V. Rudchenko and A. F. Tulinov, Soviet Physics JETP 23, 391 (1966).
BN67	6A	L. B. Bridwell, L. C. Northcliffe, S. Datz, C. D. Moak and H. O. Lutz, Phys. Rev. 159, 276 (1967).
BO48	7	N. Bohr, Dan. Mat. Fys. Medd. 18, No. 8 (1948) (ed. 2, 1953).
BO67	5	E. Bonderup, Dan. Mat. Fys. Medd. 35, No. 17 (1967).
BR59	8	E. Breitenberger, Proc. Roy. Soc. (London) A250, 514 (1959).
BR64	9	H. Breuer, Z. Phys. 180, 209 (1964).
BR68	6D	D. K. Brice, Phys. Rev. 165, 475 (1968).
BS65	10	J. W. Boring, G. E. Strohl and F. R. Woods, Phys. Rev. 140, A1065 (1965).
BS67	9	M. J. Berger and S. M. Seltzer, Paper 10 in NA67.
BS68	6B	J. P. Biersack, Z. Phys. 211, 495 (1968).
BT67	10	H. Bichsel and C. Tschalär, Nuclear Data A3, 343 (1967) and UCRL-17663.
BT68	3	H. Bichsel and C. Tschalär, Phys. Rev. 175, 476 (1968).
BU60	4,7	H. Bichsel and E. A. Uehling, Phys. Rev. 119, 1670 (1960).
BZ67	4	M. J. Berger and S. M. Seltzer, Paper 5 in NA67.

****

CA68	6B,10	G. L. Cano, Phys. Rev. 169, 277 (1968).
CB68	6A,B	W. K. Chu, P. D. Bourland, K. H. Wang, and D. Powers, Phys. Rev. 175, 342 (1968).

CC67	6A	J. B. Cumming and V. P. Crespo, Phys. Rev. 161, 287 (1967).
CS68	6B	P. D. Croft and K. Street, Jr., Phys. Rev. 165, 1375 (1968).
CT65	9	V. E. Coslett and R. N. Thomas, Brit. J. Appl. Phys., 16, 779 (1965), 15, 1283 (1964), 15, 883 (1964).

****

DA68	1	J. A. Davies, Conference Secretary, Can. J. Phys. 46, (March 15, 1968).
DB67	10	D. P. Donnelly, H. W. Baer, J. J. Reidy and M. L. Wiedenbeck, Nucl. Inst. Meth. 57, 219 (1967).
DD68	2	D. A. Dahlberg, D. K. Anderson, and I. E. Dayton, Phys. Rev. 170, 127 (1968).
DF67	10	G. Di Cola and L. Farese, Phys. Rev. 162, 690 (1967).
DK68	2	R. C. Der, T. M. Kavanagh, J. M. Khan, B. P. Curry and R. J. Fortner, Phys. Rev. Lett. 21, 1731 (1968).
DM69	6D	S. Datz, C. D. Moak, T. S. Noggle, B. R. Appleton and H. O. Lutz, Phys. Rev. 179, 315 (1969).
DR68	9	W. E. Dance, D. H. Rester, B. J. Farmer, J. H. Johnson and L. L. Baggerly, J. Appl. Phys. 39, 2881 (1968).
DT68	5	P. Dalton and J. E. Turner, Health Physics 15, 257 (1968).
DW68	6D	J. A. Davies, J. Denhartog and J. L. Whitton, Phys. Rev. 165, 345 (1968).

****

EP61	8	R. M. Eisberg and C. E. Porter, Rev. Mod. Phys. 33, 190 (1961).
ER67	6D	L. Eriksson, Phys. Rev. 161, 235 (1967).
ES69	2	H. Ehrhardt, M. Schulz, T. Tekaat, and K. Willmann, Phys. Rev. Lett. 22, 89 (1969).

****

FA47	10	U. Fano, Phys. Rev. 72, 26 (1947).

FA53 7 U. Fano, Phys. Rev. 92, 328 (1953).

FA56 3 U. Fano, Phys. Rev. 103, 1202 (1956).

FA63 2 U. Fano, Ann. Rev. Nucl. Sci. 13, 1 (1963). Reprinted in NA67.

FB68 6A B. Fastrup, A. Borup and P. Hvelplund, Canad. J. Phys. 48, 489 (1968).

FC68 2 U. Fano and J. W. Cooper, Rev. Mod. Phys. 40, 441 (1968).

FK67 10 V. Forgue and S. Kahn, Nucl. Inst. Meth. 48, 93 (1967).

FL67 1 I. P. Flaks, V International Conference of the Physics of Electronic and Atomic Collisions, Leningrad, 17-23 July, 1967. Publishing House, "Nauk" Leningrad.

FS69 10 G. Forcinal, P. Siffert and A. Coche, IEEE Trans. Nucl. Science NS15, No. 1, 475 (1968).

****

GD68 8 Yu. N. Gnedin, A. Z. Dolginov, and A. I. Tsygan, Soviet Physics JETP 27, 267 (1968).

GF59 9 K. Gubernator, and A. Flammersfeld, Z. Phys. 156, 179 (1959).

****

HA59 9 H. E. Hall, A. O. Hanson and D. Jamnik, Phys. Rev. 115, 633 (1959).

HA68 6 D. E. Harrison, Jr., Appl. Phys. Lett. 13, 277 (1968).

HF68 8 P. C. Hemmer and I. E. Farquhar, Phys. Rev. 168, 294 (1968).

HL69 6 H. H. Heckman and P. J. Lindstroem, Phys. Rev. Lett. 22, 871 (1969).

HP60 4,6 H. H. Heckman, B. L. Perkins, W. G. Simon, F. M. Smith and W. H. Barkas, Phys. Rev. 117, 544 (1960).

HR68 9 E. Hara, Nucl. Inst. Meth. 65, 85 (1968).

HU57 9 A. M. Hudson, Phys. Rev. 105, 1 (1957).

HV68 6 P. Hvelplund and B. Fastrup, Phys. Rev. 165, 408 (1968).

IS67	3	R. Ishiwari, N. Shiomi, Y. Mori, T. Onata, and Y. Uemura, Bull. Inst. Chem. Res. Kyoto Univ. 45, 379 (1967).
JA66	4	J. F. Janni, AFWL - TR - 65 - 150.
JA68	8	D. F. Jackson and C. G. Morgan, Phys. Rev. 175, 1402 (1968).
JD67	6,6B	P. Jespersgard and J. A. Davies, Can. J. Phys. 45, 2983 (1967).
JK68	3	C. H. Johnson and R. L. Kernell, Phys. Rev. 169, 974 (1968).

****

KA67	10	A. H. Krulisch and R. C. Axtmann, Nucl. Inst. Meth. 55, 238 (1967).
KA68	10	R. Katz and E. J. Kobetich, Phys. Rev. 170, 397 (1968).
KE66	9	N. D. Kessaris, Phys. Rev. 145, 164 (1966).
KE68	6B	V. S. Kessel'man, Soviet Phys. Semicond. 2, 76, (1968).
KF67	6B	S. Kahn and V. Forgue, Phys. Rev. 163, 290 (1967).
KH68	2,5	G. S. Khandelwal, Nucl. Phys. A116, 97 (1968).
KJ68	2	G. S. Khandelwal, Phys. Rev. 167, 136 (1968).
KK68	9	E. J. Kobetich and R. Katz, Phys. Rev. 170, 391 (1968).
KM61	9	G. Knop, A. Minten and B. Nellen, Z. Phys. 165, 533 (1961).
KM66	2	G. S. Khandelwal and E. Merzbacher, Phys. Rev. 144, 349 (1966).
KO64	4	L. Koschmieder, Z. Naturforsch. 19a, 1414 (1964).
KO68	7	J. J. Kolata, T. M. Amos and H. Bichsel, Phys. Rev. 176, 484 (1968).
KP52	9	L. Katz and A. S. Penfold, Rev. Mod. Phys. 24, 28 (1952).
KP67	2	J. M. Khan, D. L. Potter, R. D. Worley and H. P. Smith, Phys. Rev. 163, 81 (1967).
KY68	2	H. L. Kyle and K. Omidvar, Phys. Rev. 176, 164 (1968).

LA44	7	L. Landau, USSR Jour. Phys. 8, 201 (1944).
LB37	3	M. S. Livingston and H. Bethe, Rev. Mod. Phys. 9, 263 (1937).
LE52	4,7	H. W. Lewis, Phys. Rev. 85, 20 (1952).
LH65	10	R. Leimgruber, P. Huber, and E. Baumgartner, Helv. Phys. Acta 38, 499 (1965).
LI65	6D	Jens Lindhard, Mat. Fys. Medd. Dan. Vid. Selsk. 34, No. 14 (1965).
LN68	6B	J. Lindhard, V. Nielsen and M. Scharff, Mat. Fys. Medd. Dan. Vid. Selsk. 36, 10 (1968).
LO67	8	N. O. Lassen and A. Ohrt, Mat. Fys. Medd. Dan. Vid. Selsk 36, 9 (1967).
LP57	9	J. E. Leiss, S. Penner and C. S. Robinson, Phys. Rev. 107, 1544 (1957).
LS53	3	J. Lindhard and M. Scharff, Mat. Fys. Medd. Dan. Vid. Selsk. 27 15 (1953).
LS63	6B	J. Lindhard, M. Scharff and H. E. Schiøtt, Mat. Fys. Medd. Dan. Vid. Selsk, 33 14 (1963).
LS67	6B	L. Lehmann, H. Spehl and N. Wertz, Nucl. Inst. Meth. 55, 201 (1967).

****

MA68	3	A. H. Morton, D. A. Aldcroft and M. F. Payne, Phys. Rev. 165, 415 (1968).
MB66	6A,B	C. D. Moak and M. D. Brown, Phys. Rev. 149, 244 (1966).
ML58	2	E. Merzbacher and H. W. Lewis, Encyclopedia of Physics 34, (Springer, Berlin, 1958), p. 166.
ML68	6	C. D. Moak, H. O. Lutz, L. B. Bridwell, L. C. Northcliffe and S. Datz, Phys. Rev. 176, 427 (1968).
MO47	8	G. Moliere, Z. Naturforsch, 2A, 133 (1947).
MO48	8	G. Moliere, Z. Naturforsch 3A, 78 (1947).
MO55	8	G. Moliere, Z. Naturforsch 10A, 177 (1955).
MO58	8	R. F. Mozley, R. C. Smith and R. E. Taylor, Phys. Rev. 111, 647 (1958).

MR67	4	A. Marcinkowski, H. Rzewuski, and Z. Werner, Nucl. Inst. and Meth. 57, 338 (1967).
MR68	7	H. D. Maccabee, M. R. Raju and C. A. Tobias, Phys. Rev. 165, 469 (1968).
MS65	6B	L. Morbitzer and A. Scharmann, Z. Phys. 185, 488 (1965).
MT65	6	J. H. E. Mattauch, W. Thiele and A. H. Wapstra, Nuclear Physics 67, 1 (1965).
MY68	10	I. T. Myers, Ch. 7 "Ionization", Radiation Dosimetry, 2nd edition (Academic Press, January 1968).
MZ67	8	J. B. Marion and B. A. Zimmerman, Nucl. Inst. Meth. 51, 93 (1967).

****

NA67	1	Publication 1133, Nat. Academy Sciences - Nat. Res. Council. U. Fano, ed. 2nd printing (1967).
NI61	7	L. P. Nielsen, Mat. Fys. Medd. Dan. Vid. Selsk. 33, No. 6 (1961).
NM67	3	C. A. Nicoletta, P. J. McNulty and P. L. Jain, Phys. Rev. 164, 1693 (1967).
NO63	6A	L. C. Northcliffe, Ann. Rev. Nucl. Sci. 13, 67 (1963) Reprinted in NA67.
NO67	6	L. C. Northcliffe, Paper 8, NA67.
NS61	8	B. P. Nigam, M. K. Sundaresan and Ta-You Wu, Phys. Rev. 115, 491 (1959).
NV66	6B	D. K. Nichols and V. A. J. Van Lint, Solid State Physics 18, 1 (1966) (Advances in Research Applications, Academic Press).

****

OH63	6B	O. S. Oen, D. K. Holmes, and M. T. Robinson, J. Appl. Phys. 34, 302 (1963).
OL67	2	W. J. B. Oldham, Phys. Rev. 161, 1 (1967).
OR68	3	J. H. Ormrod, Can. J. Phys. 46, 497 (1968).

PB64	10	J. A. Phipps, J. W. Boring and R. A. Lowry, Phys. Rev. 135, A36 (1964).
PB68	6	T. E. Pierce, W. W. Bowman and M. Blann, Phys. Rev. 172, 287 (1968).
PE62	9	J. F. Perkins, Phys. Rev. 126, 1781 (1962).
PG68	10	R. H. Pehl, F. S. Goulding, D. A. Landis, and M. Lenzlinger, Nucl. Inst. and Meth. 59, 45 (1968).
PR69	10	J. M. Palms, P. V. Rao, R. E. Wood, IEEE Trans. Nucl. Science NS 16, No. 1, 36 (1969).

****

RB69	10	J. A. Ray and C. F. Barnett, IEEE Trans. Nucl. Science NS-16, No. 1, 82 (1969).
RC54	9	F. Rohrlich and B. C. Carlson, Phys. Rev. 93, 38 (1954).
RO60	6	R. G. Roll and F. E. Steiger, Nucl. Phys. 17, 54 (1960).
RO68	9	Wm. C. Roesch, "Radiation Dosimetry" Ch. 5, Vol. 1, F. H. Attix and Wm. C. Roesch, eds. (Academic Press, New York, January, 1968).
RO69	6D	M. T. Robinson, Phys. Rev. 179, 327 (1969).
RS60	6	L. C. Northcliffe, Phys. Rev. 120, 1744 (1960).
RS67	6D	J. Remillieux, J. J. Samueli, and A. Sarazin, Jour. de Phys. 28, 832 (1967).
RU68	2	M. R. H. Rudge, Rev. Mod. Phys. 40, 564 (1968).
RY55	4	B. V. Rybakov, Soviet Phys. JETP 1, 435 (1955).

****

SA65	10	A. R. Sattler, Phys. Rev. 138, A1815 (1965).
SB67	7	S. M. Seltzer and M. J. Berger, Section 9 in NA67.
SC63	8	W. T. Scott, Rev. Mod. Phys. 35, 231 (1963).
SC66	6B	H. Schiøtt, Mat. Fys. Medd. Dan. Vid. Selsk. 35, 9 (1966).

SG67	7	P. Shulek, B. M. Golovin, L.A. Kulyukina, S. V. Medved, and P. Pavlovich, Soviet J. Nucl. Phys. 4, 400 (1967).
SI67	9	J. J. Singh, NASA TN D-3927 (May 1967).
SK67	10	D. J. Skyrme, Nucl. Inst. Meth. 57, 61 (1967).
SP54	9	L. V. Spencer and U. Fano, Phys. Rev. 93, 1172 (1954).
SP55	9	L. V. Spencer, Phys. Rev. 98, 1597 (1955).
SP59	9	L. V. Spencer, Nat. Bur. Std. (U.S.) Monograph 1.
ST60	4	R. M. Sternheimer, Phys. Rev. 117, 485 (1960).
ST67	3	R. M. Sternheimer, Phys. Rev. 164, 349 (1967).
SU60	4,7	R. M. Sternheimer, Phys. Rev. 118, 1045 (1960).
SV68	6D	A. R. Sattler and F. L. Vook, Phys. Rev. 175, 526 (1968).
SY48	7	K. R. Symon, Thesis, Harvard Univ. (Cambridge, Mass. 1948).
SZ65	3	C. A. Sautter and E. J. Zimmerman, Phys. Rev. 140, A490 (1965).

****

TB68	4,8	C. Tschalär and H. Bichsel, Nucl. Inst. Meth. 62, 208 (1968).
TH52	3	T. J. Thompson, UCRL-1910.
TH67	2	E. W. Thomas, Phys. Rev. 164, 151 (1967).
TM59	8	M. L. Ter-Mikayelian, Nucl. Phys. 9, 679 (1958-1959).
TP69	6	B. N. Taylor, W. H. Parker, and D. N. Langenberg Rev. Mod. Phys. (to be published).
TS67	3,7,10	C. Tschalär, Thesis, University of Southern California (Los Angeles, January 1967).
TS68	7	C. Tschalär, Nucl. Inst. Meth. 61, 141 (1968).
TT68	4,7	C. Tschalär, Nucl. Inst. Meth. 64, 237 (1968).

VA57	7	P. V. Vavilov, Sov. Phys. JETP 5, 749 (1957).
VS68	2	L. Vriens, J. A. Simpson and S. R. Mielczarek, Phys. Rev. 165, 7 (1968), 170, 163 (1968).
VV68	9	K. J. VanCamp and V. J. Vanhuyse, Z. Phys. 211, 152 (1968).

****

WA51	2	M. C. Walske, Thesis, Cornell Univ. (1951).
WA52	2,5	M. C. Walske, Phys. Rev. 88, 1283 (1952).
WA56	2,5	M. C. Walske, Phys. Rev. 101, 940 (1950).
WH58	3	Ward Whaling, Encyclopedia of Physics, 34, 202 (1958), Springer, Berlin.
WH33	5	J. A. Wheeler, Phys. Rev. 43, 258 (1933).
WI68	6A	K. B. Winterbo Can. J. Phys. 46, 2429 (1968).
WM67	3	W. White and R. M. Mueller, J. Appl. Phys. 38, 3660 (1967).
ZM69	10	H. R. Zulliger, L. M. Middleman and D. W. Aitken, IEEE Trans. Nucl. Science, NS16, 1, 47 (1969).

Table I. Relativistic velocity $\beta = v/c$, β^2 and stopping number function $f(\beta)$ for heavy ions as a function of the kinetic energy T.

Kinetic Energy T for					β	β^2	$f(\beta)$
Protons (MeV)	Alphas (MeV)	Pions (MeV)	Muons (MeV)	Electrons (keV)			
.50	1.9863	.0744	.0563	.2723	.032634	.001065	6.9925
.55	2.1849	.0818	.0619	.2995	.034225	.001171	7.0877
.60	2.3836	.0893	.0676	.3268	.035745	.001278	7.1746
.65	2.5822	.0967	.0732	.3540	.037204	.001384	7.2546
.70	2.7808	.1041	.0788	.3812	.038606	.001490	7.3286
.75	2.9795	.1116	.0845	.4085	.039960	.001597	7.3975
.80	3.1781	.1190	.0901	.4357	.041269	.001703	7.4620
.85	3.3767	.1265	.0957	.4629	.042537	.001809	7.5225
.90	3.5753	.1339	.1014	.4902	.043769	.001916	7.5796
.95	3.7740	.1413	.1070	.5174	.044966	.002022	7.6336
1.00	3.9726	.1488	.1126	.5446	.046132	.002128	7.6848
1.10	4.3699	.1636	.1239	.5991	.048380	.002341	7.7800
1.20	4.7671	.1785	.1351	.6536	.050528	.002553	7.8668
1.30	5.1644	.1934	.1464	.7080	.052587	.002765	7.9467
1.40	5.5616	.2083	.1577	.7625	.054567	.002978	8.0206
1.50	5.9589	.2231	.1689	.8169	.056478	.003190	8.0895
1.60	6.3562	.2380	.1802	.8714	.058326	.003402	8.1539
1.70	6.7534	.2529	.1914	.9259	.060116	.003614	8.2143
1.80	7.1507	.2678	.2027	.9803	.061854	.003826	8.2713
1.90	7.5479	.2827	.2140	1.0348	.063544	.004038	8.3252
2.00	7.9452	.2975	.2252	1.0893	.065189	.004250	8.3764
2.10	8.3425	.3124	.2365	1.1437	.066794	.004461	8.4250
2.20	8.7397	.3273	.2477	1.1982	.068360	.004673	8.4714
2.30	9.1370	.3422	.2590	1.2526	.069891	.004885	8.5157
2.40	9.5342	.3570	.2703	1.3071	.071388	.005096	8.5581
2.50	9.9315	.3719	.2815	1.3616	.072855	.005308	8.5987
2.60	10.3288	.3868	.2928	1.4160	.074292	.005519	8.6378
2.70	10.7260	.4017	.3041	1.4705	.075701	.005731	8.6754
2.80	11.1233	.4165	.3153	1.5250	.077084	.005942	8.7116
2.90	11.5205	.4314	.3266	1.5794	.078442	.006153	8.7465
3.00	11.9178	.4463	.3378	1.6339	.079776	.006364	8.7803
3.10	12.3151	.4612	.3491	1.6884	.081089	.006575	8.8129
3.20	12.7123	.4760	.3604	1.7428	.082380	.006786	8.8445
3.30	13.1096	.4909	.3716	1.7973	.083650	.006997	8.8751
3.40	13.5068	.5058	.3829	1.8517	.084901	.007208	8.9048
3.50	13.9041	.5207	.3941	1.9062	.086134	.007419	8.9336
3.60	14.3014	.5356	.4054	1.9607	.087349	.007630	8.9616
3.70	14.6986	.5504	.4167	2.0151	.088547	.007841	8.9889
3.80	15.0959	.5653	.4279	2.0696	.089728	.008051	9.0154
3.90	15.4931	.5802	.4392	2.1241	.090894	.008262	9.0412
4.00	15.8904	.5951	.4505	2.1785	.092045	.008472	9.0664
4.10	16.2877	.6099	.4617	2.2330	.093181	.008683	9.0909
4.20	16.6849	.6248	.4730	2.2874	.094303	.008893	9.1148
4.30	17.0822	.6397	.4842	2.3419	.095411	.009103	9.1382
4.40	17.4794	.6546	.4955	2.3964	.096507	.009314	9.1610
4.50	17.8767	.6694	.5068	2.4508	.097589	.009524	9.1834
4.60	18.2740	.6843	.5180	2.5053	.098660	.009734	9.2052
4.70	18.6712	.6992	.5293	2.5598	.099718	.009944	9.2265
4.80	19.0685	.7141	.5405	2.6142	.100766	.010154	9.2474
4.90	19.4657	.7289	.5518	2.6687	.101802	.010364	9.2679
5.00	19.8630	.7438	.5631	2.7232	.102827	.010573	9.2879
5.50	21.8493	.8182	.6194	2.9955	.107803	.011622	9.3825
6.00	23.8356	.8926	.6757	3.2678	.112552	.012668	9.4687
6.50	25.8219	.9670	.7320	3.5401	.117102	.013713	9.5480
7.00	27.8082	1.0414	.7883	3.8124	.121474	.014756	9.6213
7.50	29.7945	1.1157	.8446	4.0847	.125688	.015797	9.6895
8.00	31.7808	1.1901	.9009	4.3570	.129758	.016837	9.7533
8.50	33.7671	1.2645	.9572	4.6294	.133699	.017875	9.8131
9.00	35.7534	1.3389	1.0135	4.9017	.137521	.018912	9.8695
9.50	37.7397	1.4133	1.0698	5.1740	.141233	.019947	9.9228

Table I (continued)

Kinetic Energy T for							
Protons (MeV)	Alphas (MeV)	Pions (MeV)	Muons (MeV)	Electrons (keV)	β	β^2	f(β)
10.00	39.7260	1.4876	1.1261	5.4463	.144845	.020980	9.9733
10.50	41.7123	1.5620	1.1824	5.7186	.148363	.022012	10.0213
11.00	43.6986	1.6364	1.2387	5.9909	.151795	.023042	10.0671
11.50	45.6849	1.7108	1.2950	6.2632	.155145	.024070	10.1108
12.00	47.6712	1.7852	1.3514	6.5356	.158420	.025097	10.1526
12.50	49.6575	1.8596	1.4077	6.8079	.161623	.026122	10.1927
13.00	51.6438	1.9339	1.4640	7.0802	.164759	.027145	10.2311
13.50	53.6301	2.0083	1.5203	7.3525	.167831	.028167	10.2681
14.00	55.6164	2.0827	1.5766	7.6248	.170844	.029188	10.3037
14.50	57.6027	2.1571	1.6329	7.8971	.173800	.030206	10.3380
15.00	59.5890	2.2315	1.6892	8.1695	.176701	.031223	10.3712
15.50	61.5753	2.3059	1.7455	8.4418	.179552	.032239	10.4032
16.00	63.5616	2.3802	1.8018	8.7141	.182353	.033253	10.4342
16.50	65.5479	2.4546	1.8581	8.9864	.185108	.034265	10.4643
17.00	67.5342	2.5290	1.9144	9.2587	.187818	.035276	10.4934
17.50	69.5205	2.6034	1.9707	9.5310	.190486	.036285	10.5216
18.00	71.5068	2.6778	2.0270	9.8033	.193112	.037292	10.5490
18.50	73.4931	2.7522	2.0833	10.0757	.195700	.038298	10.5757
19.00	75.4794	2.8265	2.1396	10.3480	.198249	.039303	10.6016
19.50	77.4657	2.9009	2.1960	10.6203	.200762	.040306	10.6269
20.00	79.4520	2.9753	2.2523	10.8926	.203241	.041307	10.6514
21.00	83.4246	3.1241	2.3649	11.4372	.208097	.043305	10.6988
22.00	87.3972	3.2728	2.4775	11.9819	.212829	.045296	10.7438
23.00	91.3698	3.4216	2.5901	12.5265	.217443	.047281	10.7868
24.00	95.3424	3.5704	2.7027	13.0711	.221947	.049261	10.8279
25.00	99.3150	3.7191	2.8153	13.6158	.226348	.051234	10.8673
26.00	103.2876	3.8679	2.9279	14.1604	.230652	.053200	10.9051
27.00	107.2602	4.0167	3.0405	14.7050	.234864	.055161	10.9414
28.00	111.2328	4.1654	3.1532	15.2496	.238989	.057116	10.9763
29.00	115.2054	4.3142	3.2658	15.7943	.243032	.059064	11.0100
30.00	119.1780	4.4629	3.3784	16.3389	.246996	.061007	11.0425
31.00	123.1506	4.6117	3.4910	16.8835	.250885	.062943	11.0738
32.00	127.1232	4.7605	3.6036	17.4282	.254704	.064874	11.1042
33.00	131.0958	4.9092	3.7162	17.9728	.258454	.066799	11.1335
34.00	135.0684	5.0580	3.8288	18.5174	.262140	.068717	11.1620
35.00	139.0410	5.2068	3.9414	19.0621	.265763	.070630	11.1896
36.00	143.0136	5.3555	4.0541	19.6067	.269327	.072537	11.2164
37.00	146.9862	5.5043	4.1667	20.1513	.272833	.074438	11.2424
38.00	150.9588	5.6531	4.2793	20.6959	.276284	.076333	11.2677
39.00	154.9314	5.8018	4.3919	21.2406	.279683	.078222	11.2923
40.00	158.9040	5.9506	4.5045	21.7852	.283030	.080106	11.3163
41.00	162.8766	6.0994	4.6171	22.3298	.286328	.081984	11.3396
42.00	166.8492	6.2481	4.7297	22.8745	.289579	.083856	11.3624
43.00	170.8218	6.3969	4.8424	23.4191	.292784	.085722	11.3845
44.00	174.7944	6.5457	4.9550	23.9637	.295944	.087583	11.4062
45.00	178.7670	6.6944	5.0676	24.5084	.299062	.089438	11.4273
46.00	182.7396	6.8432	5.1802	25.0530	.302138	.091287	11.4480
47.00	186.7122	6.9919	5.2928	25.5976	.305173	.093131	11.4682
48.00	190.6848	7.1407	5.4054	26.1422	.308170	.094969	11.4879
49.00	194.6574	7.2895	5.5180	26.6869	.311129	.096801	11.5072
50.00	198.6300	7.4382	5.6306	27.2315	.314051	.098628	11.5261
52.50	208.5615	7.8102	5.9122	28.5931	.321203	.103171	11.5716
55.00	218.4930	8.1821	6.1937	29.9547	.328147	.107680	11.6149
57.50	228.4245	8.5540	6.4752	31.3162	.334896	.112155	11.6562
60.00	238.3560	8.9259	6.7568	32.6778	.341463	.116597	11.6956
62.50	248.2875	9.2978	7.0383	34.0394	.347858	.121005	11.7333
65.00	258.2190	9.6697	7.3198	35.4010	.354091	.125380	11.7695
67.50	268.1505	10.0416	7.6014	36.7625	.360170	.129723	11.8041
70.00	278.0820	10.4135	7.8829	38.1241	.366105	.134033	11.8375
72.50	288.0135	10.7855	8.1644	39.4857	.371903	.138312	11.8696

Table I (continued)

Kinetic Energy T for							
Protons (MeV)	Alphas (MeV)	Pions (MeV)	Muons (MeV)	Electrons (keV)	β	β^2	$f(\beta)$
75.00	297.9450	11.1574	8.4460	40.8473	.377569	.142558	11.9005
77.50	307.8765	11.5293	8.7275	42.2088	.383111	.146774	11.9304
80.00	317.8080	11.9012	9.0090	43.5704	.388534	.150958	11.9592
82.50	327.7395	12.2731	9.2906	44.9320	.393843	.155112	11.9871
85.00	337.6710	12.6450	9.5721	46.2936	.399043	.159236	12.0141
87.50	347.6025	13.0169	9.8536	47.6551	.404140	.163329	12.0403
90.00	357.5340	13.3888	10.1352	49.0167	.409136	.167392	12.0657
92.50	367.4655	13.7608	10.4167	50.3783	.414036	.171426	12.0903
95.00	377.3970	14.1327	10.6982	51.7399	.418845	.175431	12.1142
97.50	387.3285	14.5046	10.9798	53.1014	.423564	.179407	12.1375
100.00	397.2600	14.8765	11.2613	54.4630	.428198	.183354	12.1601
105.00	417.1230	15.6203	11.8243	57.1862	.437222	.191163	12.2036
110.00	436.9860	16.3641	12.3874	59.9093	.445938	.198860	12.2450
115.00	456.8490	17.1080	12.9505	62.6325	.454366	.206448	12.2844
120.00	476.7120	17.8518	13.5135	65.3556	.462525	.213929	12.3220
125.00	496.5750	18.5956	14.0766	68.0788	.470431	.221305	12.3579
130.00	516.4380	19.3394	14.6397	70.8019	.478098	.228577	12.3923
135.00	536.3010	20.0833	15.2027	73.5251	.485539	.235748	12.4254
140.00	556.1640	20.8271	15.7658	76.2482	.492767	.242820	12.4572
145.00	576.0270	21.5709	16.3289	78.9714	.499793	.249793	12.4878
150.00	595.8900	22.3147	16.8919	81.6945	.506627	.256671	12.5173
155.00	615.7530	23.0586	17.4550	84.4177	.513279	.263455	12.5457
160.00	635.6161	23.8024	18.0181	87.1408	.519756	.270146	12.5733
165.00	655.4791	24.5462	18.5811	89.8640	.526067	.276747	12.5999
170.00	675.3421	25.2900	19.1442	92.5871	.532220	.283258	12.6257
175.00	695.2051	26.0339	19.7072	95.3103	.538221	.289682	12.6507
180.00	715.0681	26.7777	20.2703	98.0334	.544077	.296019	12.6749
185.00	734.9311	27.5215	20.8334	100.7566	.549793	.302273	12.6985
190.00	754.7941	28.2653	21.3964	103.4797	.555377	.308443	12.7214
195.00	774.6571	29.0092	21.9595	106.2029	.560832	.314532	12.7437
200.00	794.5201	29.7530	22.5226	108.9260	.566163	.320541	12.7655
205.00	814.3831	30.4968	23.0856	111.6492	.571377	.326471	12.7866
210.00	834.2461	31.2406	23.6487	114.3723	.576476	.332324	12.8073
215.00	854.1091	31.9845	24.2118	117.0955	.581464	.338101	12.8274
220.00	873.9721	32.7283	24.7748	119.8186	.586347	.343803	12.8471
225.00	893.8351	33.4721	25.3379	122.5418	.591128	.349432	12.8663
230.00	913.6981	34.2159	25.9010	125.2649	.595809	.354989	12.8851
235.00	933.5611	34.9597	26.4640	127.9881	.600396	.360475	12.9035
240.00	953.4241	35.7036	27.0271	130.7112	.604889	.365891	12.9215
245.00	973.2871	36.4474	27.5901	133.4344	.609294	.371239	12.9391
250.00	993.1501	37.1912	28.1532	136.1575	.613611	.376519	12.9564
255.00	1013.0131	37.9350	28.7163	138.8807	.617845	.381733	12.9734
260.00	1032.8761	38.6789	29.2793	141.6038	.621998	.386882	12.9900
265.00	1052.7391	39.4227	29.8424	144.3270	.626073	.391967	13.0063
270.00	1072.6021	40.1665	30.4055	147.0501	.630070	.396989	13.0223
275.00	1092.4651	40.9103	30.9685	149.7733	.633994	.401949	13.0380
280.00	1112.3281	41.6542	31.5316	152.4964	.637846	.406848	13.0534
285.00	1132.1911	42.3980	32.0947	155.2196	.641628	.411687	13.0686
290.00	1152.0541	43.1418	32.6577	157.9427	.645342	.416467	13.0835
295.00	1171.9171	43.8856	33.2208	160.6659	.648991	.421189	13.0982
300.00	1191.7801	44.6295	33.7838	163.3890	.652575	.425854	13.1126
310.00	1231.5061	46.1171	34.9100	168.8353	.659558	.435016	13.1409
320.00	1271.2321	47.6048	36.0361	174.2816	.666304	.443961	13.1682
330.00	1310.9581	49.0924	37.1622	179.7279	.672826	.452695	13.1948
340.00	1350.6841	50.5801	38.2884	185.1742	.679135	.461225	13.2206
350.00	1390.4101	52.0677	39.4145	190.6205	.685242	.469557	13.2458
360.00	1430.1361	53.5554	40.5406	196.0668	.691156	.477697	13.2703
370.00	1469.8621	55.0430	41.6667	201.5131	.696887	.485651	13.2942
380.00	1509.5881	56.5307	42.7929	206.9594	.702442	.493425	13.3176
390.00	1549.3141	58.0183	43.9190	212.4057	.707830	.501024	13.3404

Table I (continued)

Kinetic Energy T for							
Protons (MeV)	Alphas (MeV)	Pions (MeV)	Muons (MeV)	Electrons (keV)	β	β^2	$f(\beta)$
400.00	1589.0401	59.5060	45.0451	217.8520	.713059	.508453	13.3626
410.00	1628.7661	60.9936	46.1713	223.2983	.718135	.515717	13.3845
420.00	1668.4921	62.4813	47.2974	228.7446	.723064	.522822	13.4058
430.00	1708.2181	63.9689	48.4235	234.1909	.727854	.529772	13.4267
440.00	1747.9441	65.4566	49.5496	239.6372	.732510	.536570	13.4473
450.00	1787.6701	66.9442	50.6758	245.0835	.737036	.543223	13.4674
460.00	1827.3961	68.4319	51.8019	250.5298	.741440	.549733	13.4871
470.00	1867.1221	69.9195	52.9280	255.9761	.745724	.556105	13.5065
480.00	1906.8482	71.4071	54.0542	261.4224	.749895	.562342	13.5256
490.00	1946.5742	72.8948	55.1803	266.8687	.753956	.568450	13.5444
500.00	1986.3002	74.3824	56.3064	272.3150	.757911	.574430	13.5628
510.00	2026.0262	75.8701	57.4325	277.7613	.761765	.580286	13.5809
520.00	2065.7522	77.3577	58.5587	283.2076	.765521	.586023	13.5988
530.00	2105.4782	78.8454	59.6848	288.6539	.769183	.591643	13.6164
540.00	2145.2042	80.3330	60.8109	294.1002	.772754	.597149	13.6337
550.00	2184.9302	81.8207	61.9371	299.5465	.776237	.602545	13.6508
560.00	2224.6562	83.3083	63.0632	304.9928	.779636	.607832	13.6677
570.00	2264.3822	84.7960	64.1893	310.4391	.782953	.613015	13.6843
580.00	2304.1082	86.2836	65.3154	315.8854	.786191	.618096	13.7007
590.00	2343.8342	87.7713	66.4416	321.3317	.789353	.623078	13.7168
600.00	2383.5602	89.2589	67.5677	326.7780	.792441	.627963	13.7328
610.00	2423.2862	90.7466	68.6938	332.2243	.795458	.632753	13.7486
620.00	2463.0122	92.2342	69.8200	337.6706	.798406	.637451	13.7642
630.00	2502.7382	93.7219	70.9461	343.1169	.801287	.642060	13.7795
640.00	2542.4642	95.2095	72.0722	348.5632	.804103	.646582	13.7947
650.00	2582.1902	96.6972	73.1983	354.0095	.806857	.651018	13.8098
660.00	2621.9162	98.1848	74.3245	359.4558	.809550	.655372	13.8246
670.00	2661.6422	99.6725	75.4506	364.9021	.812185	.659644	13.8393
680.00	2701.3682	101.1601	76.5767	370.3484	.814762	.663837	13.8539
690.00	2741.0942	102.6478	77.7029	375.7947	.817284	.667954	13.8683
700.00	2780.8202	104.1354	78.8290	381.2410	.819753	.671995	13.8825
710.00	2820.5462	105.6231	79.9551	386.6873	.822170	.675963	13.8966
720.00	2860.2722	107.1107	81.0812	392.1336	.824536	.679859	13.9106
730.00	2899.9982	108.5984	82.2074	397.5799	.826853	.683686	13.9244
740.00	2939.7242	110.0860	83.3335	403.0262	.829123	.687444	13.9380
750.00	2979.4502	111.5737	84.4596	408.4725	.831346	.691136	13.9516
760.00	3019.1762	113.0613	85.5857	413.9188	.833524	.694763	13.9650
770.00	3058.9022	114.5490	86.7119	419.3651	.835659	.698326	13.9783
780.00	3098.6282	116.0366	87.8380	424.8114	.837751	.701827	13.9915
790.00	3138.3542	117.5243	88.9641	430.2577	.839802	.705268	14.0045
800.00	3178.0803	119.0119	90.0903	435.7040	.841813	.708649	14.0175
810.00	3217.8063	120.4996	91.2164	441.1503	.843785	.711973	14.0303
820.00	3257.5323	121.9872	92.3425	446.5966	.845718	.715239	14.0430
830.00	3297.2583	123.4749	93.4686	452.0429	.847615	.718451	14.0556
840.00	3336.9843	124.9625	94.5948	457.4892	.849476	.721609	14.0681
850.00	3376.7103	126.4502	95.7209	462.9355	.851301	.724714	14.0805
860.00	3416.4363	127.9378	96.8470	468.3818	.853093	.727767	14.0928
870.00	3456.1623	129.4255	97.9732	473.8281	.854851	.730770	14.1050
880.00	3495.8883	130.9131	99.0993	479.2744	.856576	.733723	14.1172
890.00	3535.6143	132.4008	100.2254	484.7207	.858270	.736628	14.1292
900.00	3575.3403	133.8884	101.3515	490.1670	.859933	.739485	14.1411
910.00	3615.0663	135.3761	102.4777	495.6133	.861566	.742297	14.1529
920.00	3654.7923	136.8637	103.6038	501.0596	.863170	.745063	14.1647
930.00	3694.5183	138.3514	104.7299	506.5059	.864745	.747785	14.1763
940.00	3734.2443	139.8390	105.8561	511.9522	.866293	.750463	14.1879
950.00	3773.9703	141.3266	106.9822	517.3985	.867813	.753099	14.1994
960.00	3813.6963	142.8143	108.1083	522.8448	.869306	.755694	14.2108
970.00	3853.4223	144.3019	109.2344	528.2911	.870774	.758248	14.2221
980.00	3893.1483	145.7896	110.3606	533.7374	.872216	.760762	14.2334
990.00	3932.8743	147.2772	111.4867	539.1837	.873634	.763237	14.2446
1000.00	3972.6003	148.7649	112.6128	544.6300	.875028	.765673	14.2556

Table II. Calculated mass stopping power S/ρ (MeV/g/cm^2) for protons.

	S/ρ						
	Be	Graphite	Water	Al	Cu	Ag	Pb
I(eV)=	64	78	66.6	166	320	475	820
T(MeV)							
10.0	37.720	40.875	46.641	33.776	27.169	23.213	17.620
10.5	36.252	39.303	44.840	32.531	26.218	22.435	17.068
11.0	34.904	37.858	43.185	31.385	25.341	21.714	16.556
11.5	33.662	36.525	41.666	30.325	24.528	21.045	16.079
12.0	32.513	35.292	40.254	29.343	23.773	20.422	15.633
12.5	31.448	34.147	38.944	28.429	23.069	19.840	15.216
13.0	30.456	33.082	37.724	27.577	22.409	19.294	14.823
13.5	29.531	32.087	36.586	26.779	21.790	18.781	14.454
14.0	28.666	31.156	35.521	26.032	21.209	18.299	14.105
14.5	27.855	30.283	34.522	25.330	20.663	17.844	13.775
15.0	27.094	29.463	33.583	24.669	20.148	17.415	13.463
15.5	26.376	28.690	32.700	24.045	19.662	17.009	13.167
16.0	25.700	27.960	31.865	23.456	19.202	16.625	12.885
16.5	25.061	27.271	31.077	22.898	18.764	16.259	12.618
17.0	24.456	26.618	30.331	22.369	18.348	15.910	12.363
17.5	23.882	25.999	29.623	21.866	17.953	15.579	12.120
18.0	23.337	25.411	28.951	21.389	17.577	15.263	11.888
18.5	22.820	24.852	28.312	20.934	17.218	14.961	11.666
19.0	22.327	24.320	27.703	20.500	16.876	14.673	11.454
19.5	21.857	23.812	27.123	20.086	16.549	14.398	11.251
20.0	21.409	23.327	26.569	19.690	16.237	14.134	11.056
21.0	20.571	22.421	25.534	18.949	15.651	13.639	10.688
22.0	19.802	21.590	24.584	18.268	15.110	13.181	10.348
23.0	19.095	20.824	23.710	17.640	14.609	12.756	10.032
24.0	18.442	20.117	22.902	17.059	14.145	12.362	9.738
25.0	17.837	19.462	22.153	16.519	13.714	11.995	9.464
26.0	17.275	18.852	21.457	16.017	13.312	11.653	9.207
27.0	16.750	18.284	20.808	15.548	12.936	11.333	8.965
28.0	16.261	17.753	20.202	15.109	12.585	11.033	8.738
29.0	15.802	17.256	19.634	14.697	12.254	10.750	8.524
30.0	15.372	16.789	19.101	14.310	11.943	10.483	8.323
31.0	14.967	16.349	18.600	13.946	11.648	10.230	8.132
32.0	14.586	15.935	18.127	13.602	11.370	9.992	7.952
33.0	14.225	15.544	17.681	13.276	11.107	9.766	7.780
34.0	13.885	15.174	17.258	12.969	10.857	9.553	7.617
35.0	13.562	14.823	16.859	12.677	10.620	9.349	7.461
36.0	13.256	14.491	16.479	12.399	10.395	9.156	7.313
37.0	12.965	14.175	16.119	12.135	10.181	8.972	7.172
38.0	12.689	13.874	15.775	11.884	9.977	8.797	7.037
39.0	12.425	13.587	15.449	11.645	9.782	8.629	6.908
40.0	12.174	13.314	15.137	11.416	9.596	8.469	6.785
41.0	11.934	13.053	14.839	11.198	9.418	8.315	6.667
42.0	11.704	12.804	14.555	10.989	9.248	8.167	6.554
43.0	11.485	12.565	14.282	10.788	9.085	8.025	6.445
44.0	11.275	12.336	14.022	10.597	8.928	7.889	6.340
45.0	11.073	12.117	13.771	10.413	8.777	7.759	6.239
46.0	10.880	11.906	13.531	10.236	8.632	7.633	6.142
47.0	10.694	11.704	13.301	10.066	8.493	7.513	6.049
48.0	10.515	11.509	13.079	9.903	8.358	7.396	5.958
49.0	10.343	11.322	12.866	9.745	8.229	7.284	5.872
50.0	10.178	11.142	12.660	9.594	8.104	7.176	5.788
52.5	9.790	10.719	12.179	9.238	7.811	6.922	5.590
55.0	9.435	10.333	11.738	8.911	7.543	6.689	5.409
57.5	9.109	9.977	11.333	8.611	7.295	6.475	5.241
60.0	8.808	9.649	10.959	8.334	7.066	6.275	5.085
62.5	8.530	9.345	10.613	8.077	6.854	6.090	4.940
65.0	8.271	9.064	10.293	7.839	6.657	5.917	4.804
67.5	8.031	8.801	9.994	7.616	6.474	5.756	4.678
70.0	7.807	8.557	9.715	7.409	6.302	5.606	4.560
72.5	7.597	8.328	9.454	7.214	6.140	5.465	4.449

Table II. Continued.

	S/ρ						
	Be	Graphite	Water	Al	Cu	Ag	Pb
I(eV)=	64	78	66.6	166	320	475	820
T(MeV)							
75.0	7.400	8.113	9.210	7.032	5.988	5.332	4.344
77.5	7.215	7.911	8.980	6.860	5.846	5.207	4.246
80.0	7.041	7.721	8.764	6.699	5.711	5.090	4.153
82.5	6.877	7.542	8.560	6.546	5.584	4.978	4.065
85.0	6.722	7.373	8.368	6.402	5.463	4.873	3.982
87.5	6.576	7.213	8.185	6.266	5.350	4.773	3.902
90.0	6.437	7.061	8.013	6.136	5.241	4.679	3.827
92.5	6.305	6.917	7.849	6.013	5.139	4.589	3.755
95.0	6.180	6.780	7.693	5.897	5.041	4.503	3.687
97.5	6.060	6.650	7.545	5.785	4.948	4.422	3.622
100.0	5.947	6.526	7.403	5.679	4.859	4.343	3.559
105.0	5.735	6.294	7.140	5.481	4.693	4.197	3.443
110.0	5.541	6.083	6.899	5.300	4.542	4.063	3.337
115.0	5.364	5.888	6.678	5.134	4.402	3.940	3.238
120.0	5.200	5.709	6.475	4.980	4.274	3.826	3.148
125.0	5.049	5.544	6.287	4.839	4.155	3.721	3.064
130.0	4.909	5.391	6.113	4.707	4.044	3.623	2.986
135.0	4.779	5.248	5.951	4.585	3.942	3.532	2.912
140.0	4.657	5.116	5.800	4.471	3.845	3.447	2.844
145.0	4.544	4.992	5.659	4.364	3.755	3.368	2.780
150.0	4.438	4.876	5.527	4.264	3.671	3.293	2.720
155.0	4.338	4.767	5.403	4.171	3.592	3.224	2.664
160.0	4.245	4.664	5.287	4.083	3.517	3.158	2.611
165.0	4.157	4.568	5.177	4.000	3.447	3.096	2.560
170.0	4.073	4.477	5.074	3.921	3.381	3.037	2.513
175.0	3.995	4.391	4.976	3.847	3.318	2.982	2.468
180.0	3.921	4.309	4.883	3.777	3.259	2.929	2.426
185.0	3.850	4.232	4.796	3.710	3.202	2.879	2.386
190.0	3.783	4.159	4.712	3.647	3.149	2.832	2.347
195.0	3.720	4.089	4.633	3.587	3.098	2.787	2.311
200.0	3.659	4.023	4.558	3.530	3.049	2.744	2.276
205.0	3.601	3.960	4.486	3.475	3.003	2.703	2.243
210.0	3.547	3.900	4.418	3.424	2.959	2.664	2.211
215.0	3.494	3.842	4.353	3.374	2.917	2.626	2.181
220.0	3.444	3.787	4.290	3.326	2.877	2.590	2.152
225.0	3.396	3.735	4.230	3.281	2.838	2.556	2.125
230.0	3.350	3.684	4.173	3.238	2.801	2.523	2.098
235.0	3.306	3.636	4.118	3.196	2.766	2.492	2.072
240.0	3.264	3.590	4.066	3.156	2.732	2.461	2.048
245.0	3.223	3.546	4.015	3.117	2.699	2.432	2.024
250.0	3.184	3.503	3.967	3.081	2.668	2.404	2.001
255.0	3.147	3.462	3.920	3.045	2.638	2.378	1.980
260.0	3.111	3.422	3.876	3.011	2.609	2.352	1.959
265.0	3.076	3.384	3.832	2.978	2.581	2.327	1.938
270.0	3.043	3.348	3.791	2.946	2.554	2.303	1.919
275.0	3.010	3.312	3.751	2.916	2.528	2.280	1.900
280.0	2.979	3.278	3.712	2.886	2.503	2.258	1.882
285.0	2.949	3.245	3.675	2.858	2.479	2.236	1.864
290.0	2.920	3.214	3.639	2.830	2.456	2.215	1.847
295.0	2.892	3.183	3.604	2.804	2.433	2.195	1.831
300.0	2.865	3.153	3.570	2.778	2.411	2.176	1.815
310.0	2.814	3.097	3.506	2.729	2.370	2.139	1.785
320.0	2.766	3.044	3.446	2.683	2.331	2.104	1.757
330.0	2.720	2.994	3.389	2.640	2.294	2.071	1.730
340.0	2.678	2.947	3.336	2.600	2.260	2.041	1.705
350.0	2.637	2.903	3.286	2.562	2.227	2.012	1.681
360.0	2.599	2.862	3.239	2.526	2.196	1.984	1.659
370.0	2.564	2.822	3.194	2.492	2.168	1.958	1.638
380.0	2.530	2.785	3.152	2.459	2.140	1.934	1.618
390.0	2.497	2.750	3.112	2.429	2.114	1.911	1.599

Table II. Continued.

	S/ρ						
	Be	Graphite	Water	Al	Cu	Ag	Pb
I(eV)=	64	78	66.6	166	320	475	820
T(MeV)							
400.0	2.467	2.717	3.074	2.400	2.089	1.889	1.581
410.0	2.438	2.685	3.038	2.372	2.066	1.868	1.564
420.0	2.410	2.655	3.004	2.346	2.044	1.848	1.548
430.0	2.384	2.626	2.971	2.321	2.022	1.829	1.533
440.0	2.359	2.598	2.940	2.297	2.002	1.811	1.518
450.0	2.335	2.572	2.910	2.275	1.983	1.794	1.504
460.0	2.313	2.547	2.882	2.253	1.964	1.778	1.491
470.0	2.291	2.524	2.855	2.232	1.947	1.762	1.478
480.0	2.270	2.501	2.829	2.213	1.930	1.747	1.466
490.0	2.250	2.479	2.804	2.194	1.914	1.733	1.454
500.0	2.231	2.458	2.780	2.176	1.898	1.719	1.443
510.0	2.213	2.438	2.758	2.158	1.884	1.706	1.432
520.0	2.195	2.419	2.736	2.142	1.870	1.693	1.422
530.0	2.179	2.400	2.715	2.126	1.856	1.681	1.412
540.0	2.162	2.383	2.695	2.111	1.843	1.670	1.403
550.0	2.147	2.366	2.676	2.096	1.830	1.659	1.394
560.0	2.132	2.349	2.657	2.082	1.818	1.648	1.385
570.0	2.118	2.334	2.639	2.068	1.807	1.638	1.377
580.0	2.104	2.319	2.622	2.055	1.796	1.628	1.369
590.0	2.091	2.304	2.606	2.043	1.785	1.618	1.361
600.0	2.078	2.290	2.590	2.030	1.775	1.609	1.353
610.0	2.065	2.277	2.574	2.019	1.765	1.600	1.346
620.0	2.054	2.263	2.560	2.007	1.755	1.592	1.339
630.0	2.042	2.251	2.545	1.997	1.746	1.584	1.333
640.0	2.031	2.239	2.531	1.986	1.737	1.576	1.326
650.0	2.020	2.227	2.518	1.976	1.728	1.568	1.320
660.0	2.010	2.216	2.505	1.966	1.720	1.561	1.314
670.0	2.000	2.205	2.493	1.957	1.712	1.554	1.308
680.0	1.990	2.194	2.481	1.948	1.704	1.547	1.303
690.0	1.981	2.184	2.469	1.939	1.697	1.540	1.297
700.0	1.972	2.174	2.458	1.930	1.690	1.534	1.292
710.0	1.963	2.165	2.447	1.922	1.683	1.528	1.287
720.0	1.955	2.155	2.437	1.914	1.676	1.522	1.282
730.0	1.947	2.146	2.426	1.906	1.669	1.516	1.277
740.0	1.939	2.138	2.417	1.899	1.663	1.510	1.273
750.0	1.931	2.129	2.407	1.892	1.657	1.505	1.268
760.0	1.924	2.121	2.398	1.885	1.651	1.500	1.264
770.0	1.916	2.113	2.389	1.878	1.645	1.495	1.260
780.0	1.909	2.106	2.380	1.871	1.640	1.490	1.256
790.0	1.903	2.098	2.372	1.865	1.634	1.485	1.252
800.0	1.896	2.091	2.363	1.859	1.629	1.480	1.248
810.0	1.890	2.084	2.355	1.853	1.624	1.476	1.245
820.0	1.883	2.077	2.348	1.847	1.619	1.471	1.241
830.0	1.877	2.071	2.340	1.841	1.614	1.467	1.238
840.0	1.871	2.064	2.333	1.836	1.610	1.463	1.235
850.0	1.866	2.058	2.326	1.830	1.605	1.459	1.231
860.0	1.860	2.052	2.319	1.825	1.601	1.455	1.228
870.0	1.855	2.046	2.312	1.820	1.596	1.451	1.225
880.0	1.850	2.040	2.306	1.815	1.592	1.448	1.222
890.0	1.845	2.035	2.299	1.811	1.588	1.444	1.220
900.0	1.840	2.029	2.293	1.806	1.585	1.441	1.217
910.0	1.835	2.024	2.287	1.801	1.581	1.437	1.214
920.0	1.830	2.019	2.282	1.797	1.577	1.434	1.212
930.0	1.826	2.014	2.276	1.793	1.574	1.431	1.209
940.0	1.821	2.009	2.270	1.789	1.570	1.428	1.207
950.0	1.817	2.005	2.265	1.785	1.567	1.425	1.204
960.0	1.813	2.000	2.260	1.781	1.563	1.422	1.202
970.0	1.809	1.996	2.255	1.777	1.560	1.419	1.200
980.0	1.805	1.991	2.250	1.773	1.557	1.417	1.198
990.0	1.801	1.987	2.245	1.770	1.554	1.414	1.196
1000.0	1.797	1.983	2.240	1.766	1.551	1.412	1.193

Table IIIA. Low energy proton stopping power S (MeV cm^2/g) for several substances. Accuracy: 2-20 % .

T(MeV)	H_2	He	Li	Be	C	N_2	O_2	Ne	Al	A	Ni	Cu	Kr	Ag	Sn	Xe	Au	Pb	Air	H_2O
.01					440				260		100	70					22			
.02					560				360		145	160					44			
.03					640				410		177	190					60			
.04					700				440		200	200					75			
.05	3800	1050		690	720	750	600	350	460	480	220	210	270			240	85		730	890
.10	3500	1090	750	700	710	780	610	440	440	480	260	220	290			230	105	122	730	910
.15	2800	960	680	640	650	690	600	440	390	430	270	220	250			210	112	127	650	830
.20	2300	830	610	570	580	610	540	420	340	380	260	220	220			192	119	127	580	740
.25	1990	740	550	510	540	530	500	390	320	330	250	210	198			176	116	120	520	660
.30	1740	660	500	460	490	480	450	360	310	300	230	200	182			163	110	113	480	600
.35	1560	600	450	430	460	440	410	340	290	270	220	192	169			152	104	106	430	540
.40	1410	550	420	390	430	400	380	320	280	250	210	183	159	151	142	143	98	100	410	500
.45	1280	510	390	370	390	370	360	300	270	230	193	175	150	142	134	134	93	95	380	460
.50	1180	480	360	350	370	350	340	290	250	220	182	168	143	134	127	127	88	90	350	430
.55	1090	450	340	330	350	320	320	270	240	210	173	161	137	128	121	121	84	86	330	400
.60	1020	420	320	310	330	310	300	260	230	200	165	155	132	122	115	115	81	83	310	380
.70	910	380	290	280	290	280	270	230	210	184	151	144	123	113	107	106	75	77	280	340
.80	810	340	260	260	270	250	250	210	197	171	141	135	116	105	100	98	70	71	260	310
.90	740	310	240	240	250	240	230	198	185	160	133	128	109	99	94	92	66	67	240	290
1.00	680	290	230	220	230	220	220	185	173	150	126	121	104	94	89	87	63	63	220	260
1.1	630	270	220	210	220	210	200	174	163	142	120	114	99	89	85	82	60	60	210	260
1.2	590	250	210	198	200	194	192	164	155	134	115	109	94	85	81	78	57	58	198	230
1.3	550	240	200	187	192	185	182	156	147	127	110	104	90	82	78	75	54	55	186	220
1.4	520	220	195	179	183	176	173	149	140	121	106	99	87	79	75	72	53	53	177	210
1.5	500	210	188	170	175	168	165	144	134	116	101	95	84	75	71	69	51	52	168	197
1.6	470	200	184	161	167	160	157	137	129	112	97	92	81	72	68	66	49	50	160	188
1.8	430	183	173	148	154	148	144	127	119	103	91	85	76	68	65	62	47	47	147	172
2.0	390	168	164	137	143	137	134	119	111	95	85	80	72	64	61	59	44	45	136	159

TABLE IIIB

EXPERIMENTAL PROTON STOPPING POWER S (MEV/GM/SQCM). FROM AH67, AS68.

T(MEV)	BE	AL	CA	SC	TI	V	CR	MN	FE	CO	NI	CU	ZN	AG	PT	AU
2.00	134.25	110.67	107.21	96.58	93.19	90.61	89.57	86.51	87.30	83.74	86.45	81.09	80.89	63.74	45.43	45.78
2.25	122.70	101.92	98.91	89.24	86.11	83.73	82.93	80.07	80.83	77.64	80.14	75.19	75.02	59.63	42.85	43.12
2.50	113.21	94.68	92.03	83.15	80.23	78.02	77.41	74.72	75.45	72.56	74.89	70.28	70.13	56.18	40.67	40.87
2.75	105.19	88.52	86.15	77.94	75.20	73.14	72.69	70.13	70.85	68.18	70.35	66.07	65.92	53.16	38.71	38.89
3.00	98.36	83.19	81.09	73.40	70.87	68.91	68.60	66.16	66.84	64.37	66.41	62.44	62.32	50.46	36.97	37.11
3.25	92.42	78.56	76.65	69.45	67.11	65.22	65.01	62.66	63.32	61.04	62.96	59.25	59.16	48.07	35.39	35.52
3.50	87.24	74.51	72.76	65.97	63.78	61.93	61.82	59.59	60.21	58.09	59.97	56.43	56.36	45.94	33.96	34.09
3.75	82.65	70.94	69.30	62.87	60.81	59.04	58.98	56.86	57.45	55.46	57.28	53.91	53.85	44.02	32.66	32.79
4.00	78.57	67.76	66.18	60.08	58.15	56.44	56.42	54.40	55.00	53.10	54.88	51.65	51.60	42.28	31.47	31.62
4.25	74.90	64.85	63.38	57.57	55.74	54.09	54.09	52.19	52.79	50.97	52.69	49.60	49.55	40.70	30.39	30.55
4.50	71.60	62.21	60.83	55.29	53.54	51.95	51.97	50.16	50.78	49.03	50.70	47.72	47.69	39.26	29.40	29.56
4.75	68.58	59.80	58.51	53.21	51.53	50.00	50.04	48.31	48.94	47.26	48.86	45.99	45.99	37.93	28.49	28.65
5.00	65.87	57.59	56.37	51.30	49.68	48.21	48.25	46.62	47.24	45.62	47.17	44.42	44.42	36.71	27.65	27.79
5.25	63.36	55.56	54.41	49.53	47.98	46.56	46.61	45.05	45.67	44.11	45.61	42.95	42.97	35.58	26.85	27.00
5.50	61.06	53.68	52.59	47.90	46.40	45.03	45.09	43.60	44.22	42.72	44.16	41.59	41.61	34.53	26.12	26.25
5.75	58.93	51.93	50.91	46.38	44.93	43.61	43.68	42.25	42.87	41.41	42.82	40.33	40.36	33.55	25.43	25.56
6.00	56.96	50.31	49.35	44.97	43.56	42.29	42.37	40.99	41.60	40.20	41.57	39.15	39.19	32.63	24.79	24.91
6.50	53.42	47.38	46.53	42.41	41.10	39.90	39.98	38.72	39.31	38.00	39.30	37.01	37.07	30.97	23.60	23.72
7.00	50.34	44.81	44.04	40.17	38.92	37.80	37.89	36.71	37.28	36.06	37.29	35.12	35.19	29.48	22.54	22.67
7.50	47.62	42.52	41.83	38.17	36.99	35.93	36.02	34.92	35.47	34.33	35.51	33.44	33.52	28.14	21.58	21.73
8.00	45.21	40.47	39.85	36.38	35.27	34.26	34.35	33.32	33.85	32.78	33.90	31.93	32.01	26.94	20.72	20.85
8.50	43.05	38.64	38.08	34.77	33.71	32.75	32.85	31.86	32.39	31.37	32.45	30.57	30.65	25.85	19.94	20.06
9.00	41.10	36.97	36.47	33.31	32.30	31.39	31.49	30.57	31.06	30.09	31.14	29.33	29.41	24.86	19.22	19.34
9.50	39.34	35.46	35.00	31.98	31.02	30.15	30.25	29.38	29.85	28.92	29.95	28.21	28.29	23.95	18.56	18.67
10.00	37.74	34.08	33.66	30.76	29.84	29.01	29.11	28.28	28.74	27.85	28.84	27.17	27.26	23.11	17.95	18.06
10.50	36.27	32.82	32.43	29.65	28.77	27.97	28.06	27.28	27.72	26.87	27.83	26.22	26.30	22.34	17.39	17.49
11.00	34.93	31.66	31.30	28.61	27.77	27.01	27.10	26.35	26.78	25.96	26.89	25.35	25.42	21.62	16.88	16.97
11.50	33.69	30.58	30.25	27.66	26.85	26.12	26.21	25.49	25.90	25.12	26.02	24.54	24.61	20.96	16.39	16.48
12.00	32.54	29.58	29.28	26.77	26.00	25.30	25.37	24.69	25.09	24.33	25.21	23.78	23.85	20.34	15.93	16.02

Table IV. Calculated csda ranges R (g/cm^2) for protons of kinetic energy T.

T(MeV)	R Be	 Graphite	 Water	 Al	 Cu	 Ag	 Pb
1.0	.0029	.0039	.0039	.0042	.0061	.0080	.0116
1.1	.0034	.0043	.0043	.0048	.0070	.0091	.0133
1.2	.0039	.0048	.0047	.0054	.0078	.0103	.0151
1.3	.0044	.0053	.0051	.0061	.0088	.0115	.0169
1.4	.0050	.0059	.0056	.0068	.0098	.0128	.0188
1.5	.0055	.0064	.0061	.0075	.0108	.0141	.0208
1.6	.0062	.0070	.0066	.0083	.0118	.0154	.0228
1.7	.0068	.0076	.0071	.0091	.0129	.0168	.0248
1.8	.0075	.0083	.0077	.0099	.0141	.0183	.0270
1.9	.0082	.0089	.0083	.0108	.0153	.0198	.0291
2.0	.0089	.0096	.0089	.0117	.0165	.0213	.0314
2.1	.0097	.0104	.0095	.0126	.0178	.0229	.0336
2.2	.0105	.0111	.0101	.0136	.0190	.0245	.0360
2.3	.0113	.0119	.0108	.0146	.0204	.0262	.0384
2.4	.0121	.0127	.0115	.0156	.0218	.0279	.0408
2.5	.0130	.0135	.0122	.0166	.0232	.0296	.0433
2.6	.0139	.0143	.0130	.0177	.0246	.0314	.0458
2.7	.0148	.0152	.0137	.0188	.0261	.0332	.0484
2.8	.0158	.0161	.0145	.0200	.0276	.0351	.0511
2.9	.0167	.0170	.0153	.0211	.0291	.0370	.0538
3.0	.0177	.0180	.0161	.0223	.0307	.0390	.0565
3.1	.0188	.0189	.0170	.0236	.0323	.0409	.0593
3.2	.0198	.0199	.0178	.0248	.0340	.0430	.0621
3.3	.0209	.0209	.0187	.0261	.0357	.0450	.0650
3.4	.0220	.0220	.0196	.0274	.0374	.0471	.0680
3.5	.0232	.0230	.0205	.0287	.0392	.0493	.0709
3.6	.0243	.0241	.0215	.0301	.0409	.0515	.0740
3.7	.0255	.0252	.0225	.0315	.0428	.0537	.0771
3.8	.0267	.0263	.0234	.0329	.0446	.0559	.0802
3.9	.0279	.0275	.0245	.0344	.0465	.0582	.0834
4.0	.0292	.0287	.0255	.0358	.0484	.0605	.0866
4.1	.0305	.0299	.0265	.0373	.0504	.0629	.0899
4.2	.0318	.0311	.0276	.0389	.0524	.0653	.0932
4.3	.0331	.0323	.0287	.0404	.0544	.0677	.0965
4.4	.0345	.0336	.0298	.0420	.0564	.0702	.0999
4.5	.0359	.0349	.0309	.0436	.0585	.0727	.1034
4.6	.0373	.0362	.0321	.0453	.0606	.0753	.1069
4.7	.0387	.0375	.0332	.0469	.0628	.0778	.1104
4.8	.0402	.0389	.0344	.0486	.0649	.0805	.1140
4.9	.0416	.0403	.0356	.0503	.0672	.0831	.1176
5.0	.0432	.0417	.0369	.0521	.0694	.0858	.1213
5.5	.0510	.0490	.0433	.0612	.0810	.0997	.1403
6.0	.0595	.0569	.0502	.0709	.0934	.1145	.1603
6.5	.0686	.0653	.0575	.0812	.1066	.1302	.1814
7.0	.0782	.0742	.0653	.0922	.1205	.1466	.2035
7.5	.0884	.0837	.0736	.1038	.1351	.1639	.2267
8.0	.0992	.0937	.0824	.1160	.1504	.1820	.2508
8.5	.1106	.1042	.0915	.1288	.1664	.2008	.2759
9.0	.1225	.1152	.1012	.1421	.1831	.2205	.3019
9.5	.1349	.1266	.1112	.1561	.2005	.2409	.3289

Table IV. Continued.

T(MeV)	R						
	Be	Graphite	Water	Al	Cu	Ag	Pb
10.0	.1479	.1386	.1217	.1706	.2186	.2620	.3568
10.5	.1614	.1511	.1327	.1857	.2373	.2840	.3856
11.0	.1755	.1641	.1440	.2013	.2567	.3066	.4154
11.5	.1901	.1775	.1558	.2175	.2768	.3300	.4460
12.0	.2052	.1915	.1680	.2343	.2975	.3541	.4776
12.5	.2208	.2059	.1807	.2516	.3188	.3790	.5100
13.0	.2370	.2207	.1937	.2695	.3408	.4045	.5433
13.5	.2536	.2361	.2072	.2879	.3635	.4308	.5775
14.0	.2708	.2519	.2211	.3068	.3867	.4578	.6125
14.5	.2885	.2682	.2353	.3263	.4106	.4855	.6484
15.0	.3067	.2849	.2500	.3463	.4351	.5138	.6851
15.5	.3254	.3021	.2651	.3668	.4602	.5429	.7226
16.0	.3446	.3198	.2806	.3879	.4860	.5726	.7610
16.5	.3643	.3379	.2965	.4095	.5123	.6030	.8002
17.0	.3845	.3564	.3128	.4316	.5393	.6341	.8403
17.5	.4052	.3755	.3295	.4542	.5668	.6659	.8811
18.0	.4264	.3949	.3465	.4773	.5950	.6983	.9228
18.5	.4481	.4148	.3640	.5009	.6237	.7314	.9652
19.0	.4702	.4351	.3819	.5251	.6530	.7651	1.0085
19.5	.4929	.4559	.4001	.5497	.6830	.7995	1.0525
20.0	.5160	.4771	.4187	.5748	.7135	.8346	1.0974
21.0	.5637	.5209	.4571	.6266	.7762	.9066	1.1894
22.0	.6132	.5663	.4970	.6804	.8412	.9812	1.2845
23.0	.6646	.6135	.5385	.7361	.9086	1.0584	1.3826
24.0	.7179	.6624	.5814	.7937	.9781	1.1380	1.4838
25.0	.7731	.7129	.6258	.8533	1.0499	1.2201	1.5880
26.0	.8301	.7651	.6717	.9148	1.1240	1.3047	1.6952
27.0	.8889	.8190	.7190	.9782	1.2002	1.3918	1.8052
28.0	.9495	.8745	.7678	1.0434	1.2786	1.4812	1.9182
29.0	1.0119	.9317	.8180	1.1106	1.3591	1.5730	2.0341
30.0	1.0760	.9904	.8696	1.1795	1.4418	1.6672	2.1529
31.0	1.1420	1.0508	.9227	1.2503	1.5266	1.7638	2.2744
32.0	1.2096	1.1127	.9772	1.3229	1.6135	1.8627	2.3988
33.0	1.2791	1.1763	1.0330	1.3974	1.7025	1.9640	2.5259
34.0	1.3502	1.2414	1.0903	1.4736	1.7935	2.0675	2.6558
35.0	1.4231	1.3081	1.1489	1.5516	1.8867	2.1733	2.7885
36.0	1.4977	1.3763	1.2089	1.6313	1.9818	2.2814	2.9239
37.0	1.5740	1.4461	1.2703	1.7129	2.0791	2.3918	3.0620
38.0	1.6520	1.5174	1.3330	1.7961	2.1783	2.5043	3.2027
39.0	1.7316	1.5903	1.3971	1.8811	2.2795	2.6191	3.3462
40.0	1.8129	1.6646	1.4625	1.9679	2.3827	2.7361	3.4922
41.0	1.8959	1.7405	1.5292	2.0563	2.4879	2.8553	3.6409
42.0	1.9805	1.8178	1.5972	2.1465	2.5951	2.9766	3.7922
43.0	2.0668	1.8967	1.6666	2.2383	2.7042	3.1002	3.9461
44.0	2.1546	1.9770	1.7373	2.3319	2.8152	3.2258	4.1025
45.0	2.2441	2.0588	1.8092	2.4271	2.9282	3.3537	4.2615
46.0	2.3353	2.1421	1.8825	2.5239	3.0431	3.4836	4.4231
47.0	2.4280	2.2268	1.9570	2.6224	3.1599	3.6157	4.5871
48.0	2.5223	2.3129	2.0329	2.7226	3.2786	3.7498	4.7537
49.0	2.6182	2.4006	2.1099	2.8244	3.3992	3.8861	4.9228
50.0	2.7156	2.4896	2.1883	2.9278	3.5216	4.0244	5.0943
52.5	2.9661	2.7184	2.3897	3.1934	3.8359	4.3792	5.5339
55.0	3.2263	2.9560	2.5988	3.4690	4.1617	4.7466	5.9886
57.5	3.4960	3.2023	2.8156	3.7545	4.4988	5.1266	6.4583
60.0	3.7752	3.4571	3.0400	4.0496	4.8470	5.5188	6.9426
62.5	4.0637	3.7204	3.2718	4.3544	5.2063	5.9233	7.4415
65.0	4.3614	3.9921	3.5111	4.6686	5.5764	6.3398	7.9547
67.5	4.6681	4.2720	3.7576	4.9922	5.9573	6.7682	8.4821
70.0	4.9839	4.5602	4.0113	5.3251	6.3487	7.2083	9.0235
72.5	5.3086	4.8563	4.2722	5.6671	6.7507	7.6601	9.5786

Table IV. Continued.

T(MeV)	R Be	 Graphite	 Water	 Al	 Cu	 Ag	 Pb
75.0	5.642	5.161	4.540	6.018	7.163	8.123	10.147
77.5	5.984	5.473	4.815	6.378	7.586	8.598	10.729
80.0	6.335	5.792	5.097	6.747	8.018	9.083	11.325
82.5	6.694	6.120	5.386	7.124	8.461	9.580	11.933
85.0	7.062	6.455	5.681	7.511	8.914	10.088	12.555
87.5	7.438	6.798	5.983	7.905	9.376	10.606	13.189
90.0	7.822	7.149	6.292	8.309	9.848	11.135	13.836
92.5	8.215	7.506	6.607	8.720	10.330	11.675	14.495
95.0	8.615	7.871	6.929	9.140	10.821	12.225	15.167
97.5	9.024	8.244	7.257	9.568	11.322	12.785	15.852
100.0	9.440	8.623	7.592	10.004	11.832	13.355	16.548
105.0	10.297	9.404	8.279	10.901	12.879	14.527	17.976
110.0	11.184	10.212	8.992	11.828	13.962	15.738	19.452
115.0	12.101	11.047	9.729	12.787	15.081	16.988	20.973
120.0	13.048	11.910	10.489	13.776	16.233	18.276	22.539
125.0	14.024	12.799	11.273	14.795	17.420	19.601	24.150
130.0	15.029	13.713	12.080	15.843	18.640	20.963	25.803
135.0	16.061	14.654	12.909	16.919	19.893	22.361	27.499
140.0	17.121	15.619	13.760	18.024	21.177	23.794	29.236
145.0	18.208	16.608	14.633	19.156	22.493	25.262	31.015
150.0	19.322	17.622	15.527	20.315	23.840	26.763	32.833
155.0	20.462	18.659	16.442	21.500	25.217	28.298	34.691
160.0	21.627	19.720	17.378	22.712	26.623	29.865	36.587
165.0	22.817	20.803	18.334	23.950	28.059	31.464	38.521
170.0	24.032	21.909	19.309	25.212	29.524	33.095	40.492
175.0	25.272	23.037	20.304	26.500	31.017	34.757	42.500
180.0	26.536	24.186	21.319	27.812	32.538	36.449	44.544
185.0	27.823	25.357	22.352	29.147	34.086	38.171	46.622
190.0	29.133	26.549	23.404	30.507	35.661	39.922	48.735
195.0	30.466	27.761	24.474	31.889	37.262	41.702	50.882
200.0	31.821	28.994	25.562	33.294	38.888	43.510	53.063
205.0	33.199	30.247	26.668	34.722	40.541	45.346	55.276
210.0	34.598	31.519	27.791	36.171	42.218	47.210	57.521
215.0	36.018	32.811	28.932	37.643	43.920	49.100	59.798
220.0	37.460	34.122	30.089	39.135	45.646	51.018	62.106
225.0	38.922	35.451	31.262	40.649	47.396	52.961	64.444
230.0	40.404	36.799	32.452	42.183	49.169	54.930	66.813
235.0	41.907	38.165	33.659	43.737	50.965	56.924	69.211
240.0	43.429	39.549	34.880	45.312	52.784	58.943	71.638
245.0	44.971	40.951	36.118	46.906	54.625	60.987	74.094
250.0	46.531	42.370	37.371	48.520	56.489	63.054	76.578
255.0	48.111	43.806	38.639	50.152	58.373	65.145	79.090
260.0	49.709	45.258	39.921	51.804	60.279	67.260	81.630
265.0	51.325	46.727	41.219	53.473	62.206	69.397	84.196
270.0	52.960	48.213	42.531	55.161	64.154	71.557	86.789
275.0	54.612	49.714	43.857	56.867	66.121	73.739	89.408
280.0	56.282	51.232	45.197	58.591	68.109	75.943	92.052
285.0	57.968	52.765	46.551	60.332	70.116	78.169	94.722
290.0	59.672	54.313	47.918	62.090	72.143	80.416	97.416
295.0	61.392	55.876	49.299	63.865	74.188	82.683	100.135
300.0	63.129	57.455	50.693	65.657	76.253	84.971	102.877
310.0	66.651	60.655	53.520	69.289	80.437	89.608	108.434
320.0	70.236	63.912	56.397	72.984	84.692	94.322	114.081
330.0	73.883	67.225	59.323	76.741	89.017	99.113	119.818
340.0	77.588	70.591	62.297	80.558	93.410	103.978	125.641
350.0	81.352	74.010	65.318	84.434	97.868	108.914	131.548
360.0	85.171	77.479	68.383	88.365	102.389	113.920	137.535
370.0	89.045	80.998	71.492	92.352	106.973	118.993	143.601
380.0	92.972	84.565	74.644	96.392	111.616	124.131	149.744
390.0	96.951	88.178	77.836	100.484	116.317	129.333	155.960

Table IV. Continued.

	R						
T(MeV)	Be	Graphite	Water	Al	Cu	Ag	Pb
400.0	100.980	91.837	81.070	104.626	121.075	134.597	162.249
410.0	105.058	95.540	84.342	108.818	125.889	139.921	168.607
420.0	109.183	99.286	87.653	113.057	130.756	145.304	175.033
430.0	113.355	103.074	91.000	117.342	135.675	150.743	181.525
440.0	117.572	106.902	94.384	121.673	140.644	156.237	188.081
450.0	121.832	110.770	97.803	126.048	145.663	161.785	194.699
460.0	126.136	114.677	101.256	130.465	150.731	167.384	201.378
470.0	130.481	118.621	104.742	134.924	155.844	173.035	208.115
480.0	134.866	122.602	108.261	139.423	161.003	178.734	214.909
490.0	139.291	126.619	111.812	143.962	166.207	184.482	221.758
500.0	143.754	130.670	115.393	148.539	171.453	190.276	228.662
510.0	148.255	134.755	119.005	153.154	176.741	196.115	235.618
520.0	152.792	138.873	122.645	157.805	182.070	201.999	242.624
530.0	157.365	143.023	126.314	162.492	187.439	207.925	249.681
540.0	161.972	147.205	130.011	167.213	192.846	213.893	256.785
550.0	166.614	151.417	133.735	171.967	198.291	219.902	263.937
560.0	171.288	155.658	137.486	176.755	203.773	225.951	271.134
570.0	175.994	159.929	141.262	181.574	209.290	232.038	278.375
580.0	180.732	164.228	145.063	186.425	214.842	238.162	285.660
590.0	185.501	168.555	148.889	191.306	220.428	244.323	292.987
600.0	190.299	172.908	152.739	196.216	226.047	250.520	300.355
610.0	195.126	177.288	156.612	201.156	231.697	256.751	307.763
620.0	199.982	181.693	160.508	206.124	237.380	263.017	315.211
630.0	204.865	186.124	164.426	211.119	243.093	269.315	322.696
640.0	209.775	190.579	168.365	216.140	248.835	275.645	330.218
650.0	214.712	195.057	172.326	221.188	254.607	282.006	337.776
660.0	219.675	199.559	176.308	226.262	260.406	288.397	345.369
670.0	224.662	204.083	180.309	231.360	266.234	294.819	352.996
680.0	229.675	208.630	184.330	236.482	272.088	301.269	360.657
690.0	234.711	213.198	188.371	241.628	277.968	307.747	368.349
700.0	239.770	217.787	192.430	246.797	283.874	314.253	376.074
710.0	244.853	222.396	196.507	251.989	289.805	320.785	383.829
720.0	249.957	227.026	200.603	257.202	295.760	327.344	391.614
730.0	255.084	231.676	204.715	262.437	301.739	333.928	399.428
740.0	260.231	236.344	208.845	267.693	307.741	340.537	407.270
750.0	265.400	241.031	212.991	272.969	313.765	347.170	415.140
760.0	270.589	245.737	217.154	278.265	319.812	353.827	423.037
770.0	275.797	250.460	221.332	283.581	325.880	360.507	430.960
780.0	281.025	255.201	225.526	288.916	331.968	367.209	438.909
790.0	286.272	259.959	229.736	294.269	338.078	373.933	446.882
800.0	291.537	264.733	233.960	299.640	344.207	380.679	454.880
810.0	296.821	269.524	238.198	305.029	350.355	387.445	462.902
820.0	302.122	274.330	242.451	310.435	356.523	394.232	470.946
830.0	307.440	279.152	246.717	315.858	362.709	401.039	479.013
840.0	312.775	283.989	250.997	321.297	368.913	407.864	487.102
850.0	318.127	288.841	255.290	326.752	375.134	414.709	495.212
860.0	323.494	293.708	259.596	332.223	381.373	421.572	503.343
870.0	328.878	298.588	263.914	337.710	387.628	428.454	511.494
880.0	334.276	303.483	268.245	343.211	393.900	435.352	519.665
890.0	339.690	308.391	272.588	348.727	400.188	442.268	527.855
900.0	345.119	313.312	276.943	354.257	406.492	449.200	536.064
910.0	350.562	318.246	281.309	359.802	412.810	456.149	544.291
920.0	356.019	323.193	285.686	365.359	419.144	463.113	552.536
930.0	361.489	328.151	290.075	370.930	425.492	470.093	560.798
940.0	366.973	333.123	294.474	376.514	431.854	477.088	569.077
950.0	372.470	338.105	298.883	382.111	438.230	484.098	577.373
960.0	377.981	343.100	303.303	387.720	444.619	491.122	585.684
970.0	383.503	348.105	307.733	393.341	451.022	498.160	594.012
980.0	389.038	353.122	312.173	398.974	457.437	505.211	602.354
990.0	394.585	358.149	316.622	404.619	463.865	512.276	610.711
1000.0	400.143	363.187	321.081	410.275	470.305	519.354	619.083

Table V. Properties of charged particles (BB69, TP69, MT65. Electron masses to be divided by 1000).

Ion	z	Lifetime	Charge	Mass			m_r
		nano sec	10^{-19}C	10^{-24}g	amu	MeV	
ELECTRON	1	STABLE	±1.60219	0.910956	0.548593	511.004	0.544630
MUON	1	2198.3	±1.60219	0.188357	0.113432	105.6598	0.112613
PION	1	26.04	±1.60219	0.248823	0.149846	139.578	0.148763
KAON	1	12.35	±1.60219	0.880322	0.530147	493.82	0.526317
SIGMA+	1	0.081	+1.60219	2.120318	1.276895	1189.40	1.267671
SIGMA-	1	0.164	-1.60219	2.134436	1.285398	1197.32	1.276112
		Mass excess MeV					
1N	0	8.0714	0.	1.674920	1.0086652	939.553	1.0013786
1H	1	7.2890	1.60219	1.672614	1.0072766	938.259	1.0000000
2H	1	13.1359	1.60219	3.343569	2.0135536	1875.587	1.9990076
3H	1	14.9500	1.60219	5.007334	3.0155011	2808.883	2.9937170
3HE	2	14.9313	3.20438	5.006390	3.0149325	2808.353	2.9931526
4HE	2	2.4248	3.20438	6.644626	4.0015059	3727.328	3.9725990
6LI	3	14.0884	4.80658	9.985570	6.0134789	5601.443	5.9700375
7LI	3	14.9073	4.80658	11.647561	7.0143581	6533.743	6.9636862
7BE	4	15.7689	6.40877	11.648186	7.0147345	6534.093	6.9640599
9BE	4	11.3505	6.40877	14.961372	9.0099911	8392.637	8.9449027
10B	5	12.0522	8.01096	16.622243	10.0101958	9324.309	9.9378820
11B	5	8.6677	8.01096	18.276741	11.0065623	10252.406	10.9270507
12C	6	0.	9.61315	19.920910	11.9967084	11174.708	11.9100440
13C	6	3.1246	9.61315	21.587011	13.0000629	12109.314	12.9061502
14C	6	3.0198	9.61315	23.247356	13.9999504	13040.691	13.8988145
14N	7	2.8637	11.21534	23.246166	13.9992342	13040.024	13.8981035
15N	7	.1004	11.21534	24.901771	14.9962676	13968.741	14.8879343
16O	8	-4.7365	12.81753	26.552769	15.9905263	14894.875	15.8750105
17O	8	-.8077	12.81753	28.220304	16.9947441	15830.285	16.8719738
18O	8	-.7824	12.81753	29.880881	17.9947713	16761.791	17.8647767
19F	9	-1.4860	14.41973	31.539247	18.9934674	17692.058	18.8562582
20NE	10	-7.0415	16.02192	33.188963	19.9869546	18617.472	19.8425685
21NE	10	-5.7299	16.02192	34.851833	20.9883627	19550.265	20.8367424
22NE	10	-8.0249	16.02192	36.508273	21.9858989	20479.451	21.8270724
23NA	11	-9.5283	17.62411	38.165213	22.9837363	21408.918	22.8177014
24MG	12	-13.9333	19.22630	39.816981	23.9784587	22335.483	23.8052379
25MG	12	-13.1907	19.22630	41.478836	24.9792559	23267.707	24.7988053
26MG	12	-16.2142	19.22630	43.133977	25.9760100	24196.165	25.7883589
27AL	13	-17.1961	20.82849	44.791847	26.9744073	25126.153	26.7795437
28SI	14	-21.4899	22.43068	46.443813	27.9692490	26052.830	27.7671987
29SI	14	-21.8936	22.43068	48.103625	28.9688156	26983.907	28.7595444
30SI	14	-24.4394	22.43068	49.759617	29.9660826	27912.843	29.7496071
31P	15	-24.4376	24.03288	51.419241	30.9655359	28843.815	30.7418404
32S	16	-26.0127	25.63507	53.076053	31.9632963	29773.210	31.7323930
33S	16	-26.5826	25.63507	54.735569	32.9626845	30704.121	32.7245615
34S	16	-29.9335	25.63507	56.390126	33.9590871	31632.251	33.7137661
36S	16	-30.6550	25.63507	59.709903	35.9583126	33494.492	35.6985491
35CL	17	-29.0145	27.23726	58.051385	34.9595251	32564.140	34.7069770
37CL	17	-31.7648	27.23726	61.367545	36.9565725	34424.353	36.6895976
36AR	18	-30.2316	28.83945	59.708836	35.9576699	33493.894	35.6979111
38AR	18	-34.7182	28.83945	63.021900	37.9528533	35352.369	37.6786813
40AR	18	-35.0383	28.83945	66.342392	39.9525096	37215.012	39.6638921
39K	19	-33.8033	30.44164	64.683151	38.9532869	36284.254	38.6718877
40K	19	-33.5333	30.44164	66.344164	39.9535768	37216.006	39.6649515
40CA	20	-34.8476	32.04383	66.340910	39.9516172	37214.180	39.6630060

Table VI. B of Moliere's theory for z= 1, 2 and 6, variable β and thickness s. For any value of z at β=0, B is the same as for z=1. The theory is valid only for B 4.5. Linear interpolation for Z or β^2 will give sufficient accuracy. Logarithmic interpolation is required for s.

Z	s				z=1						z=2		z=6	
	g/cm^2	β^2= 0	0.005	0.01	0.02	0.05	0.1	0.2	0.5	1.0	0.1	1.0	0.1	1.0
3	10^{-3}	10.5	8.8	8.3	7.6	6.6	5.7	4.9	3.8	2.8	7.4	4.6	-	-
	10^{-2}	13.0	11.5	10.8	10.2	9.2	8.5	7.7	6.6	5.7	10.0	7.4	-	-
	10^{-1}	15.4	14.0	13.3	12.8	11.7	11.0	10.3	9.2	8.5	12.5	10.0	-	-
	1	17.9	16.4	15.8	15.2	14.2	13.5	12.8	11.8	11.0	14.9	12.6	-	-
10	10^{-3}	8.2	8.0	7.7	7.4	6.7	6.0	5.2	4.2	3.2	7.2	4.9	8.1	7.2
	10^{-2}	10.7	10.5	10.3	9.9	9.25	8.7	8.0	7.0	6.2	9.8	7.7	10.6	9.7
	10^{-1}	13.3	13.0	12.8	12.4	11.8	11.2	10.5	9.6	8.8	12.3	10.3	1311	12.3
	1	15.7	15.4	15.2	14.8	14.3	13.7	13.1	12.1	11.4	14.8	12.8	15.5	14.7
20	10^{-3}	6.8	6.7	6.6	6.5	6.2	5.8	5.2	4.2	3.5	6.5	5.0	6.8	6.4
	10^{-2}	9.4	9.3	9.3	9.2	8.9	8.5	7.9	7.1	6.4	9.2	7.8	9.4	9.1
	10^{-1}	12.0	11.9	11.8	11.7	11.4	11.0	10.5	9.7	9.0	11.7	10.3	11.9	11.6
	1	14.4	14.4	14.3	14.2	13.9	13.5	13.1	12.2	11.5	14.2	12.8	14.4	14.2
50	10^{-3}	4.7	4.7	4.7	4.6	4.6	4.5	4.3	3.7	3.2	4.6	4.1	4.7	4.6
	10^{-2}	7.5	7.5	7.5	7.4	7.4	7.3	7.2	6.6	6.0	7.5	7.0	7.5	7.4
	10^{-3}	10.0	10.0	10.0	10.0	10.0	9.9	9.7	9.2	8.8	10.0	9.6	10.1	10.0
	1	12.5	12.5	12.5	12.5	12.5	12.4	12.2	11.8	11.3	12.6	12.1	12.5	12.5
100	10^{-3}	3.1	3.1	3.1	3.1	3.0	3.0	3.0	2.8	2.5	3.1	2.9	3.1	3.1
	10^{-2}	6.0	6.0	6.0	6.0	6.0	5.9	5.9	5.7	5.4	6.0	5.8	6.0	6.0
	10^{-1}	8.7	8.7	8.7	8.7	8.7	8.6	8.6	8.4	8.2	8.7	8.5	8.7	8.7
	1	11.2	11.2	11.2	11.2	11.2	11.1	11.1	10.9	10.7	11.2	11.0	11.2	11.2

TABLE VII. MULTIPLE SCATTERING DIFFERENTIAL DISTRIBUTION FUNCTION F(X) (FROM MZ67).

B=	4	5	6	7	8	9	10	12
X								
0	1.0	1.0	1.0	1.0	1.0	1.0	1.0	1.0
.2	.94070	.94546	.94850	.95058	.95208	.95321	.95409	.95537
.4	.78389	.79992	.81017	.81721	.82232	.82616	.82916	.83351
.6	.58102	.60800	.62535	.63731	.64601	.65259	.65772	.66520
.8	.38726	.41889	.43939	.45363	.46402	.47192	.47811	.48716
1.0	.23800	.26632	.28491	.29793	.30752	.31486	.32063	.32913
1.2	.14139	.16116	.17437	.18377	.19077	.19616	.20045	.20681
1.4	.08650	.09681	.10393	.10911	.11304	.11612	.11859	.12231
1.6	.05666	.05986	.06226	.06410	.06556	.06673	.06769	.06918
1.8	.03899	.03840	.03816	.03807	.03805	.03806	.03809	.03817
2.0	.02685	.02506	.02387	.02303	.02240	.02192	.02154	.02097
2.2	.01793	.01628	.01507	.01416	.01345	.01288	.01241	.01170
2.4	.01164	.01048	.00956	.00883	.00824	.00775	.00735	.00673
2.6	.00799	.00716	.00646	.00589	.00543	.00504	.00471	.00419
2.8	.00549	.00489	.00438	.00396	.00361	.00332	.00308	.00269
3.0	.00397	.00349	.00310	.00277	.00251	.00229	.00211	.00182
3.2	.00300	.00259	.00227	.00202	.00181	.00164	.00150	.00128
3.4	.00232	.00198	.00171	.00151	.00135	.00122	.00111	.00094
3.6	.00182	.00154	.00132	.00116	.00103	.00093	.00084	.00071
3.8	.00145	.00121	.00103	.00090	.00080	.00072	.00065	
4.0	.00115	.00096	.00082	.00071	.00063	.00056	.00051	
4.2	.00093	.00077	.00065	.00057	.00050	.00045	.00041	
4.4	.00075	.00062	.00053	.00046	.00041	.00037	.00033	
4.6	.00062	.00051	.00043	.00038	.00033	.00030	.00027	
4.8	.00051	.00042	.00036	.00031	.00027	.00025	.00022	
5.0	.00043	.00035	.00030	.00026	.00023	.00021	.00019	
5.2	.00036	.00030	.00025	.00022	.00019	.00018	.00016	
5.4	.00030	.00025	.00021	.00019	.00016	.00015	.00013	
5.6	.00026	.00021	.00018	.00016	.00014	.00013		
5.8	.00022	.00019	.00016	.00014	.00012	.00011		
6.0	.00019	.00016	.00014	.00012	.00010	.00010		

TABLE VIII. MULTIPLE SCATTERING INTEGRAL DISTRIBUTION FUNCTION. GIVEN IS THE FRACTION OF INCIDENT PARTICLES FOUND INSIDE A CONE OF HALF ANGLE X.

B= / X	4	5	6	7	8	9	10	12
.2	.04617	.04431	.04320	.04247	.04195	.04153	.04123	.04078
.4	.16893	.16330	.15993	.15773	.15616	.15485	.15393	.15253
.6	.33004	.32259	.31815	.31523	.31316	.31132	.31008	.30814
.8	.48890	.48427	.48156	.47981	.47856	.47716	.47637	.47496
1.0	.61973	.62202	.62359	.62473	.62554	.62555	.62592	.62614
1.2	.71612	.72641	.73300	.73759	.74088	.74266	.74449	.74676
1.4	.78446	.80062	.81102	.81829	.82357	.82679	.82981	.83380
1.6	.83429	.85269	.86473	.87324	.87948	.88340	.88704	.89194
1.8	.87231	.88987	.90159	.90998	.91620	.92011	.92378	.92875
2.0	.90166	.91679	.92709	.93457	.94016	.94358	.94690	.95136
2.2	.92375	.93623	.94485	.95118	.95591	.95868	.96149	.96519
2.4	.93964	.94997	.95714	.96242	.96636	.96849	.97080	.97375
2.6	.95110	.95983	.96584	.97026	.97353	.97513	.97700	.97928
2.8	.95964	.96714	.97224	.97596	.97869	.97985	.98136	.98308
3.0	.96607	.97259	.97697	.98014	.98244	.98325	.98447	.98575
3.2	.97115	.97684	.98062	.98334	.98528	.98581	.98680	.98772
3.4	.97529	.98024	.98351	.98584	.98750	.98779	.98860	.98924
3.6	.97872	.98302	.98584	.98786	.98927	.98938	.99002	.99043
3.8	.98158	.98531	.98776	.98950	.99071	.99066	.99117	.99140
4.0	.98398	.98722	.98934	.99086	.99189	.99172	.99212	.99224
4.2	.98600	.98882	.99067	.99199	.99288	.99260	.99291	.99296
4.4	.98771	.99018	.99179	.99295	.99372	.99334	.99357	.99359
4.6	.98917	.99134	.99275	.99377	.99443	.99397	.99413	.99413
4.8	.99043	.99233	.99357	.99447	.99504	.99452	.99462	.99461
5.0	.99152	.99320	.99429	.99508	.99557	.99500	.99504	.99503
5.2	.99247	.99395	.99491	.99561	.99603	.99541	.99541	.99541
5.4	.99331	.99461	.99545	.99607	.99644	.99578	.99573	.99574
5.6	.99405	.99519	.99594	.99648	.99680	.99610	.99602	.99604
5.8	.99470	.99571	.99637	.99685	.99712	.99639	.99628	.99631
6.0	.99530	.99618	.99676	.99719	.99741	.99666	.99651	.99655
7.0	.99655	.99720	.99762	.99793	.99810	.99755	.99744	.99747
8.0	.99736	.99785	.99818	.99842	.99854	.99812	.99804	.99806
9.0	.99791	.99830	.99856	.99875	.99885	.99852	.99845	.99847
10.0	.99831	.99863	.99883	.99899	.99907	.99880	.99874	.99876

Table IX

Critical energy T_c and Radiation length X_o for various substances (H. A. Bethe and J. Ashkin, Experimental Nuclear Physics, Vol. I, p. 166; John Wiley and Sons, New York, 1952).

Substance	T_c (MeV)	X_o (g/cm^2)
Hydrogen	340	58
Helium	220	85
Carbon	103	42.5
Nitrogen	87	38
Oxygen	77	34.2
Aluminum	47	23.9
Argon	34.5	19.4
Iron	24.	13.8
Copper	21.5	12.8
Lead	6.9	5.8
Air	83	36.5
Water	93	35.9

Table X

The comparison of maximum electron ranges R_{max} with Spencer's X_{max}. Positrons of 0.1 MeV are indicated by 0.1 . Experimental ranges from GF59; csda ranges from BS67; X_{max} is the value at which J(X) reaches a value of 0.001 (SP59).

T (MeV)	R_{max} exp.	csda range	ratio	Spencer's X_{max}	R_{max} exp.	csda range	ratio	Spencer's X_{max}
		Aluminum				Copper		
0.05	5.05	5.71	0.884	0.875	5.42	6.90	0.786	0.775
0.10	15.44	18.64	0.829	0.875	17.1	22.1	0.772	0.775
0.10-	14.4	17.3	0.832	-	16.1	20.7	0.778	-
0.15	31.0	36.4	0.850	0.875	34.0	42.8	0.795	0.760
		Silver				Gold		
0.05	5.04	7.99	0.63	0.70	4.73	9.88	0.48	-
0.10	15.6	25.2	0.62	0.67	14.3	30.3	0.47	0.57
0.10-	16.5	23.5	0.70	-	18.5	28.2	0.66	-
0.15	30.2	48.4	0.62	0.65	27.6	57.5	0.48	-

Table XI

Average energy w for the formation of an ion pair for various particles.

Particle	β	p	α	Fission fragments	
				light	heavy
T (MeV) ≅	0.3	1	5	90	60
Gas					
H_2	36.6		36.2		
He	41.5		46.0		
N_2	34.6	36.6	36.39		
O_2	31.8	31.5	32.3		
Ne	36.2	28.6	35.7		
A	26.2	26.4	26.3	28.0	29.5
Kr	24.3		24.0		
Xe	21.9		22.8		
air	33.7	36.0	34.98		
CO_2	32.9	34.9	34.1		
CH_4	27.3		29.1		
C_2H_2	25.7		27.3		
C_2H_4	26.3		28.03		
C_2H_6	24.6		26.6		
C_3H_8	27.8				
C_4H_{10}	23.0		24.8		
C_6H_{14}	22.4				
BF_3			35.6		
NH_3	34.8		30.5		
C_2H_5OH			32.6		
$C\ Cl_2F_2$			29.5		
$S\ O_2$			32.5		
H_2O	30.1		37.6		

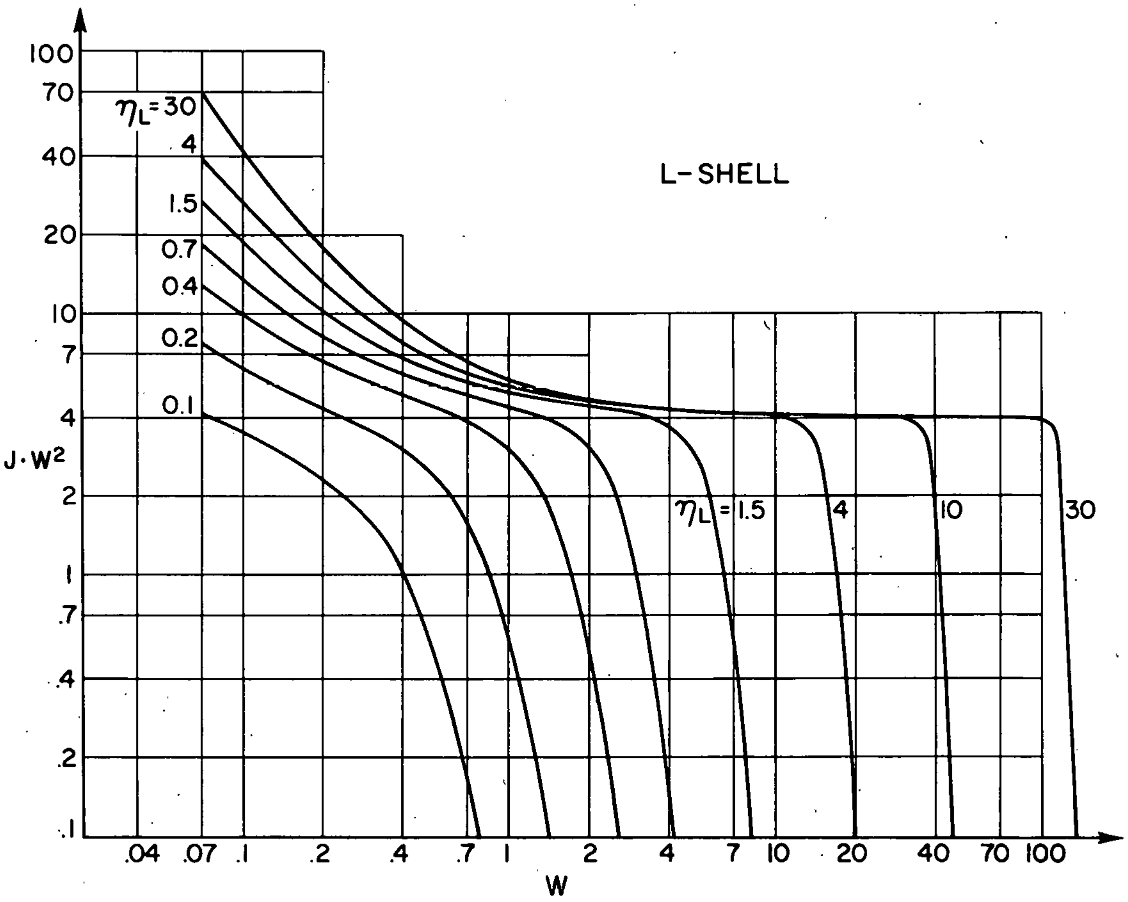

XBL.696-659

Fig. 1. First Born approximation of the excitation function J for L-shell electrons relative to free electron excitation function $J'=1/W^2$. Plotted is $J/J' = J\,W^2$ as a function of δ-ray energy $W = E/\left[13.6\text{eV}(Z - 4.15)^2\right]$. The "ionization" energy $W_{min} \cong I_L$ is approximately 0.09 for Al, 0.17 for Pb. The matrix elements are calculated with hydrogenic wave functions. In Bohr's papers, the rise at small W is described as a resonance effect.

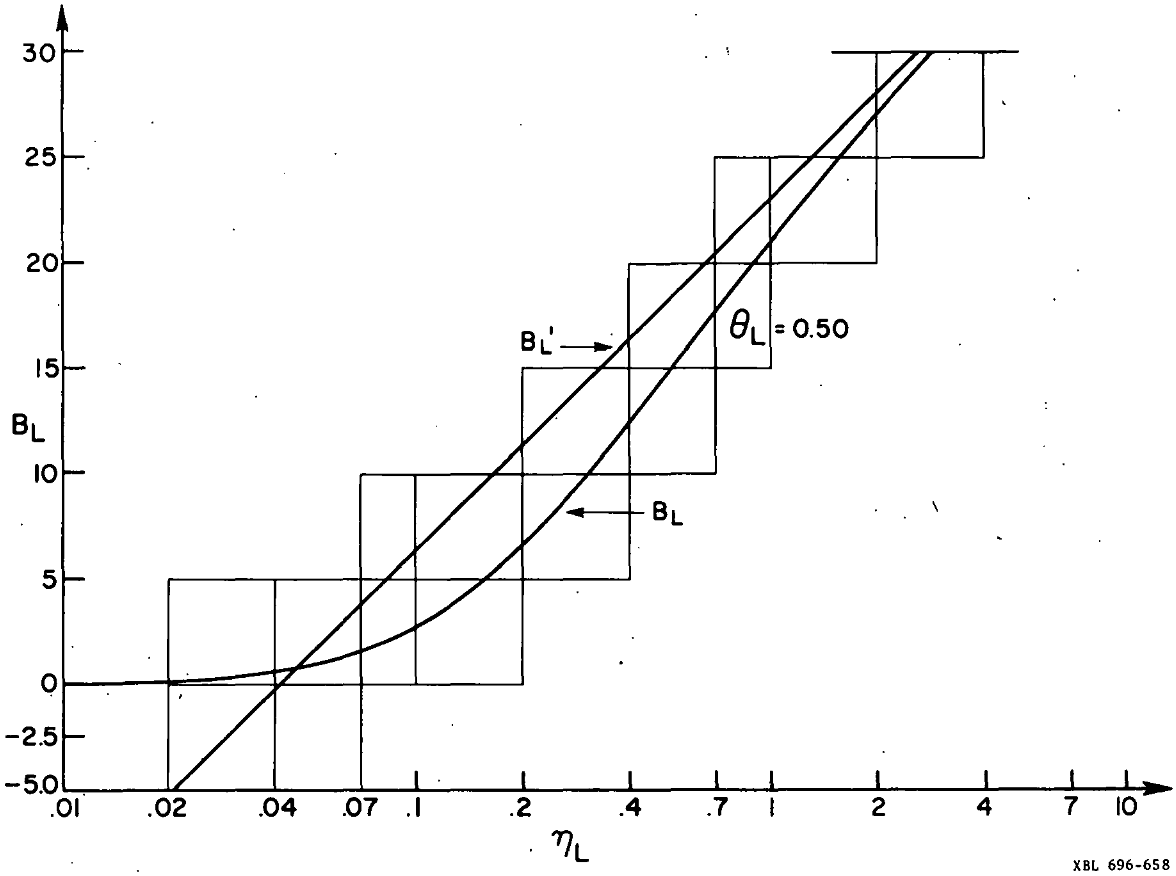

Fig. 2. The stopping number $B = \int W J \, dW$ for L-shell electrons in copper. Also given is the asymptotic expression $B' = S_L' \ln(2mv^2/I_L)$. The difference between the two functions is the shell correction C , **Eq.** (3-3); it is a basic part of the quantum mechanical theory.

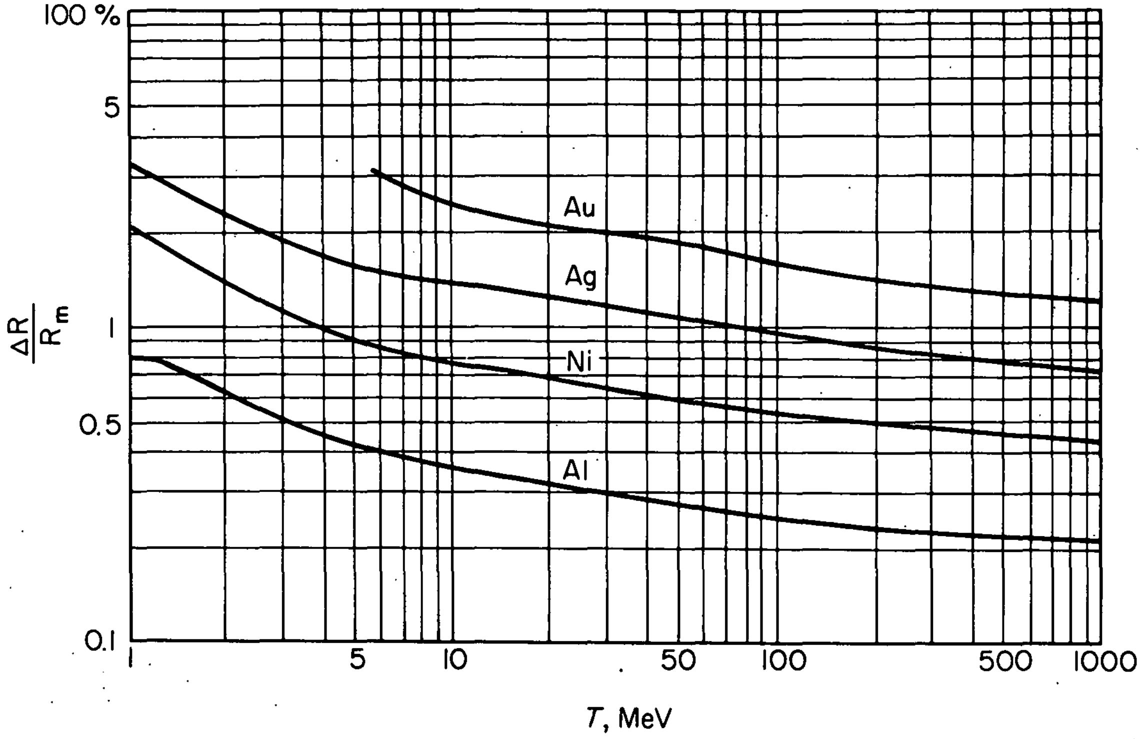

XBL 696-654

Fig. 3. The fractional multiple-scattering correction for different elements as a function of proton energy T. The experimental median projected range R_m is related to the csda range R_o through $R_o = R_m + \Delta R$. Corrections due to nuclear diffraction scattering are neglected. Accuracy 10 to 20%.

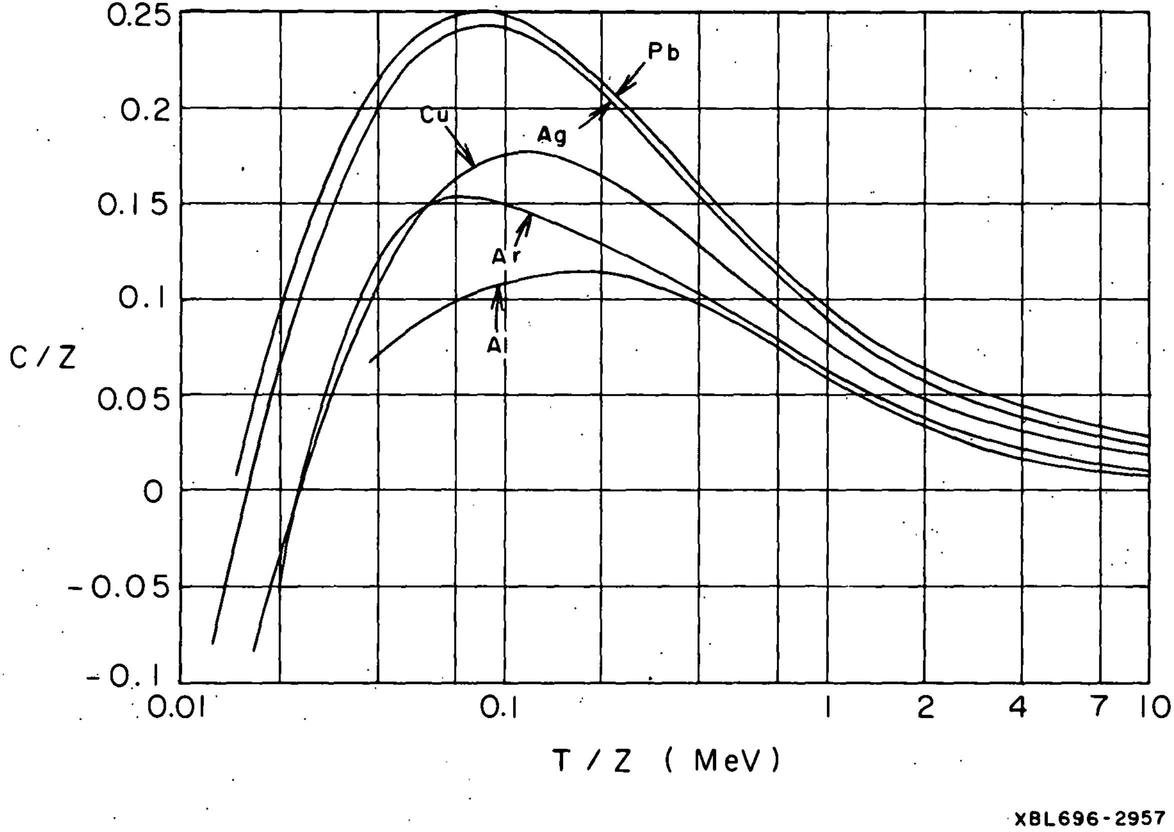

Fig. 4. Practical shell corrections C/Z for particles of charge +1. The abscissa is $T/Z = T_1/(m_r Z)$, see Eq. (3-8). For $Z \le 25$, Walske's, and for $Z > 25$, Bonderup's shell corrections are modified to fit experimental data for protons and deuterons. In this procedure, deviations from the first Born approximation are included in C/Z, and the shell corrections depend on the incident particle charge z. For $C/Z < -0.1$, the Bonderup corrections do not fit the data well.

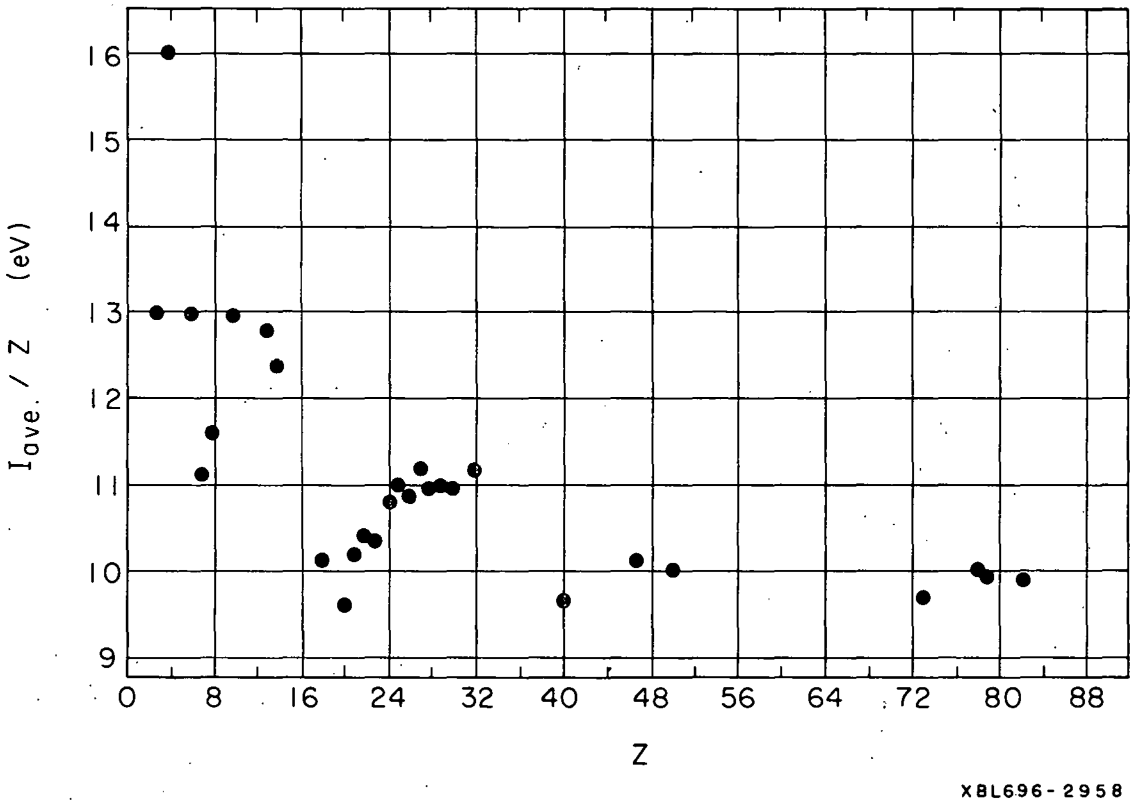

Fig. 5. The mean excitation energy I_{ave} for different elements. Given is I_{ave}/Z versus Z. For H_2, $I_{ave} = 19.2$ eV, for He, $I_{ave} = 41.3$ eV, from α-particle measurements. The values represent the authors present opinion, and may change by several percent. The strong fluctuations found for neighboring elements are significant though.

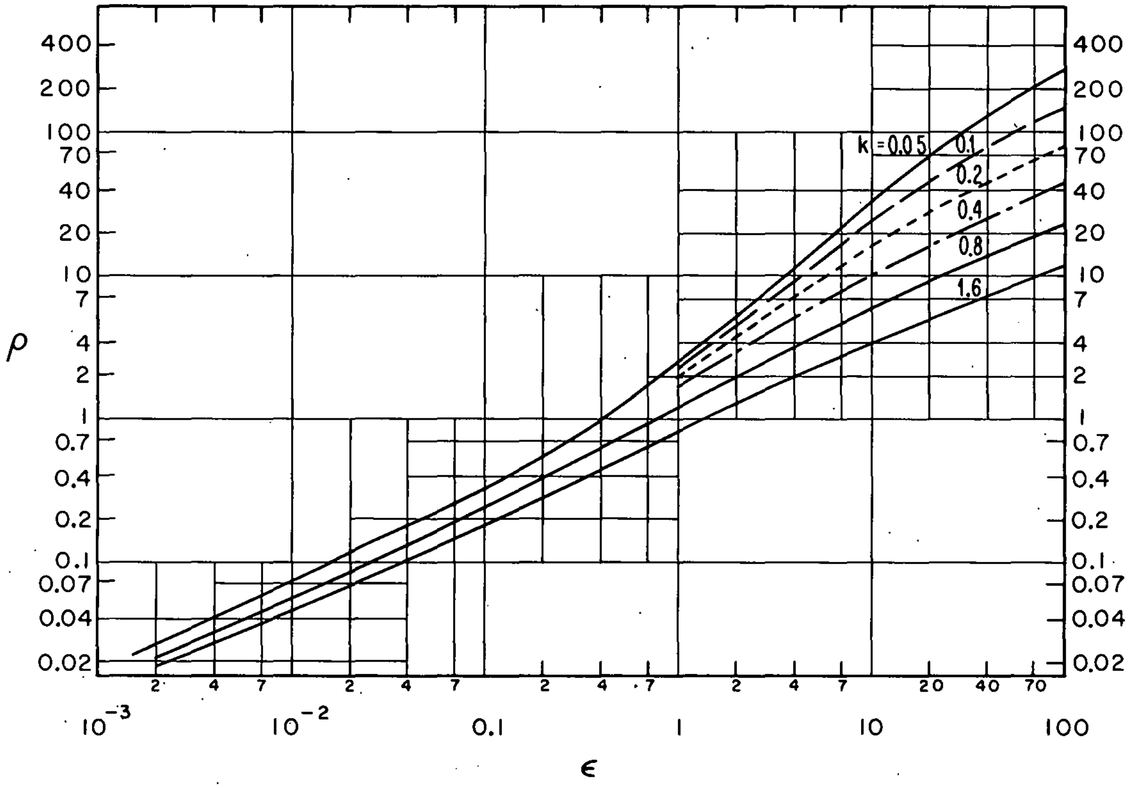

XBL695-2763

Fig. 6. Range-energy relation for low energy ions. The dimension less parameters ϵ (for the kinetic energy) and ρ (for the range) are defined in Eqs. (6-4) and (6-5). The parameter k, Eq. (6-8), is related to the low energy electronic stopping power.

Fig. 7. Contour lines for the straggling distribution function Φ $\left[\Phi(\Delta_u) = \int_0^{\Delta_u} f(\Delta) ds \text{ where } f(\Delta) \text{ is the Vavilov function}\right]$ in silicon for particles of velocity $\beta^2 = 0.04$ (T ~ 20 MeV for protons). The curves are similar for other velocities. The Vavilov theory has been modified for the quantum mechanical corrections. The Vavilov parameter is

$$\varkappa_V = 7.49 \cdot 10^{-2} s z^2 (1-\beta^2)/\beta^4$$

(for silicon; s in g/cm^2). Plotted is the energy loss p (dimension less) which exceeds the energy loss of Φ% of the incident particles. The actual energy loss is $\Delta = \bar{\Delta} + p\sigma$ where $\bar{\Delta}$ is the mean energy loss ($\bar{\Delta} = sS$), and σ is the standard deviation

$$\sigma^2 = 78{,}250 \; s \; z^2 \; (1 - \beta^2/2)/(1 - \beta^2) \quad \text{keV}^2$$

Example: 40 MeV protons, $s = 0.02$ g/cm^2, $\beta^2 = 0.08$, $\varkappa_V = 0.22$, $\bar{\Delta} = 0.02 \cdot 11.72 = 0.234$ MeV , $\sigma = 40$ KeV. For $\Delta = \bar{\Delta}$, $p = 0$, and about 58% of all the protons lose less than 234 keV. The exact answer is 61.6%. On the other hand, for $\Phi = 96\%$, $p \sim 2.0$ and $\Delta = 234 + 80$ keV = 314 keV. Thus, 4% of the protons lose more than 314 keV (the exact answer is 315 keV).

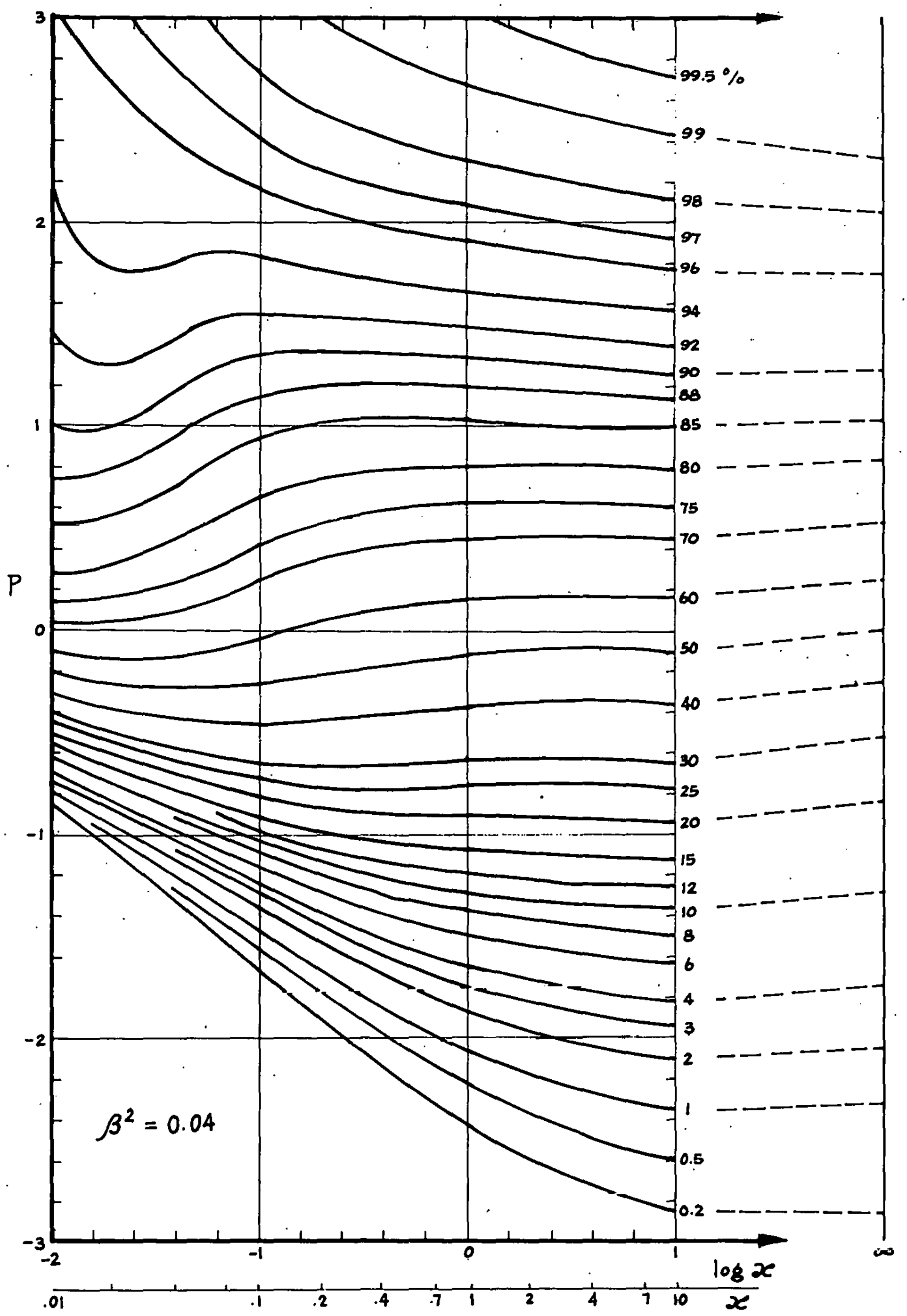
P
3
2
1
0
-1
-2
-3
-2
-1
0
1
log x
.01
.1
.2
.4
.7
1
2
4
7
10
x
∞
99.5 %
99
98
97
96
94
92
90
88
85
80
75
70
60
50
40
30
25
20
15
12
10
8
6
4
3
2
1
0.5
0.2
$\beta^2 = 0.04$

XBL 696-755

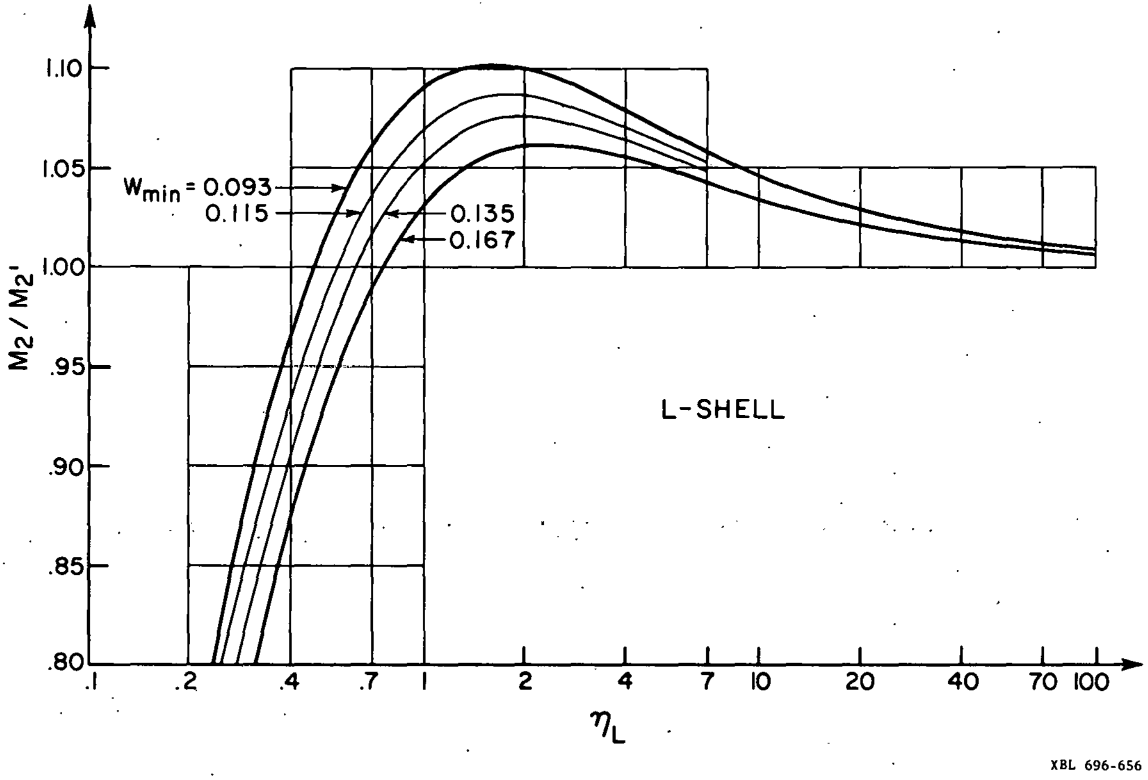

Fig. 8. The ratio M_2/M_2' of the second moments of the quantum mechanical, Eq. (2-2), and the free electron cross sections, Eq. (2-1), for the L-shell. The curves apply for silicon (W_{min} = 0.093), copper (0.115) Silver (0.135) and lead (0.167).

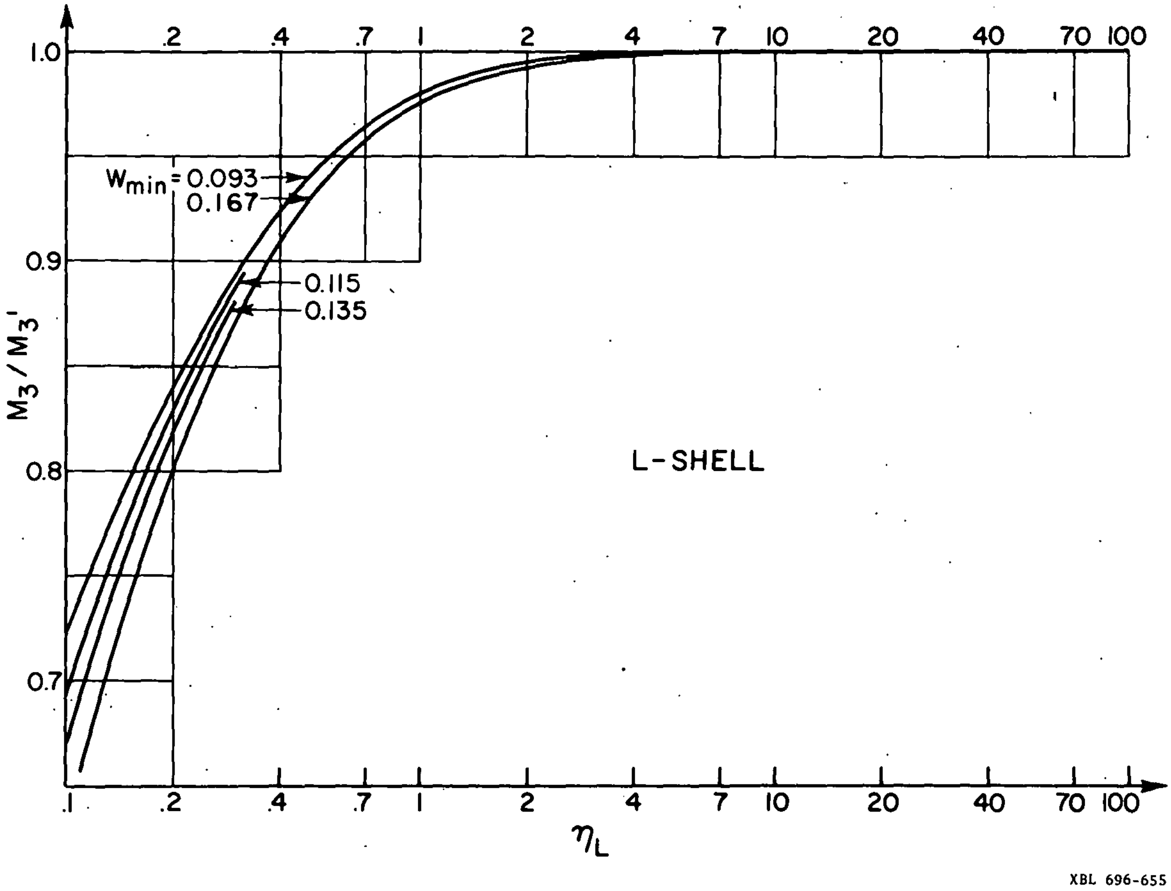

Fig. 9. The ratio M_3/M_3' of the third moments for the L-shell (see Fig. 8 for the elements). Notice that the asymmetry (skewness) is reduced at lower energies.

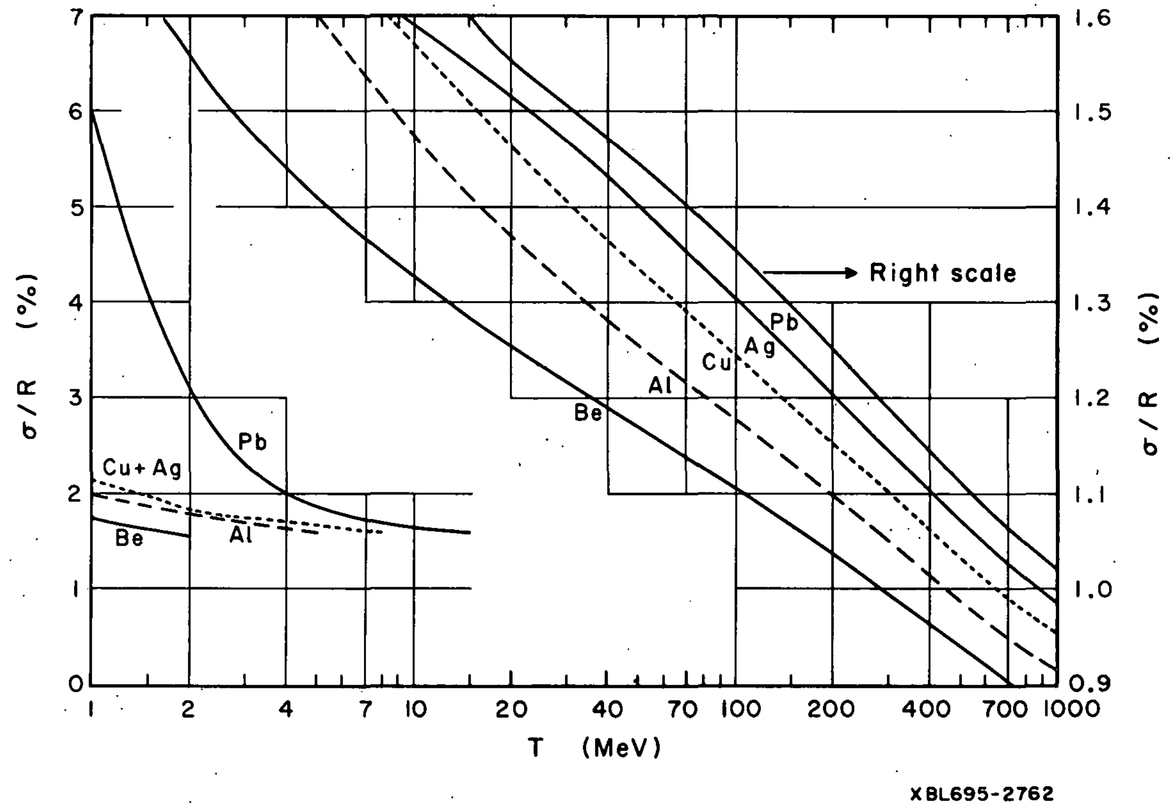

Fig. 10. The range straggling parameter σ /R (%) for protons of kinetic energy T in different elements. σ /R is corrected for the quantum mechanical effects (estimated from Fig. 8).

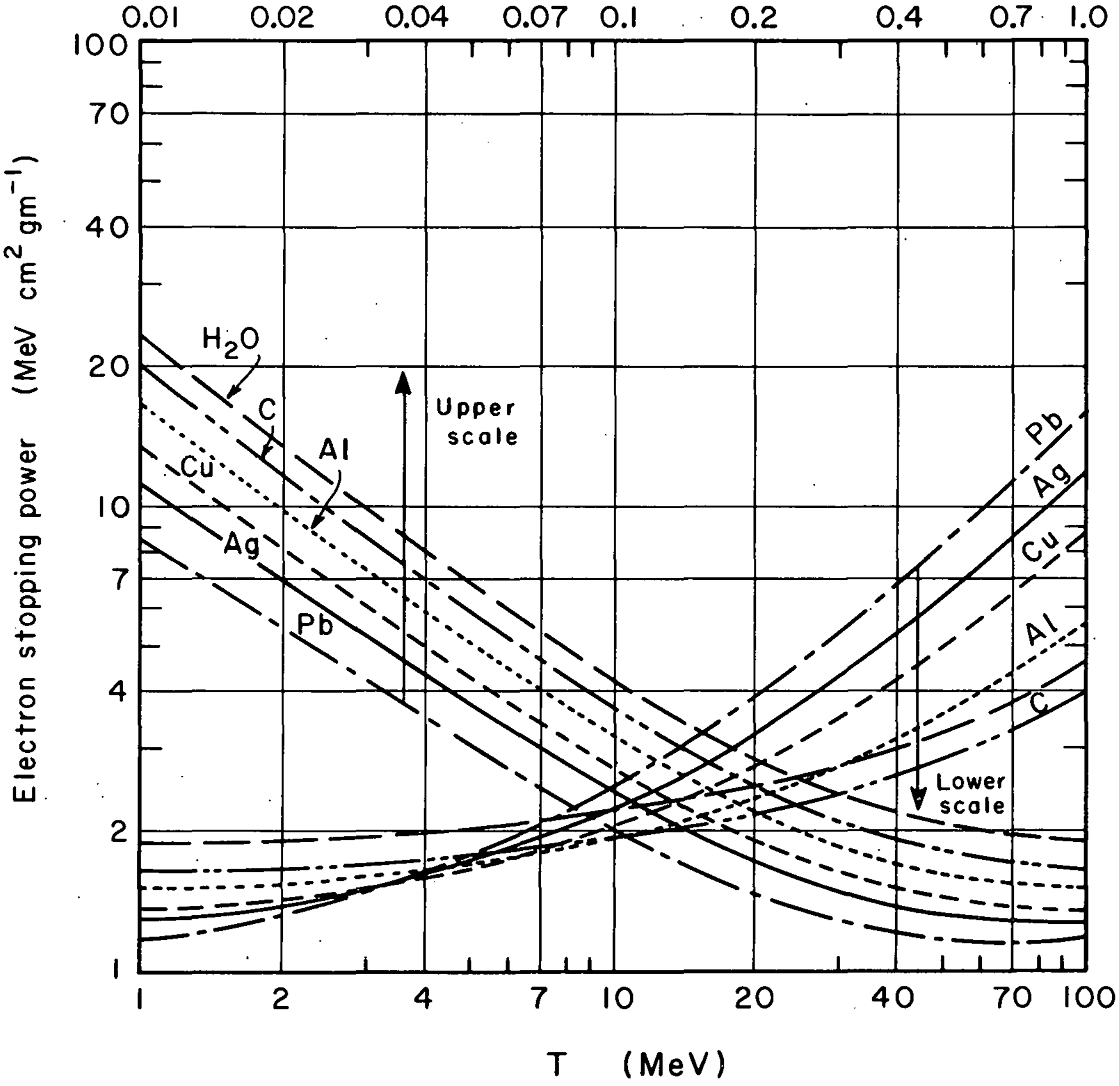

XBL695-2764

Fig. 11. Calculated electron mass stopping power S , including collision and radiation loss for different materials (BS67). The stopping power for Na I is within 1% of S for Ag.

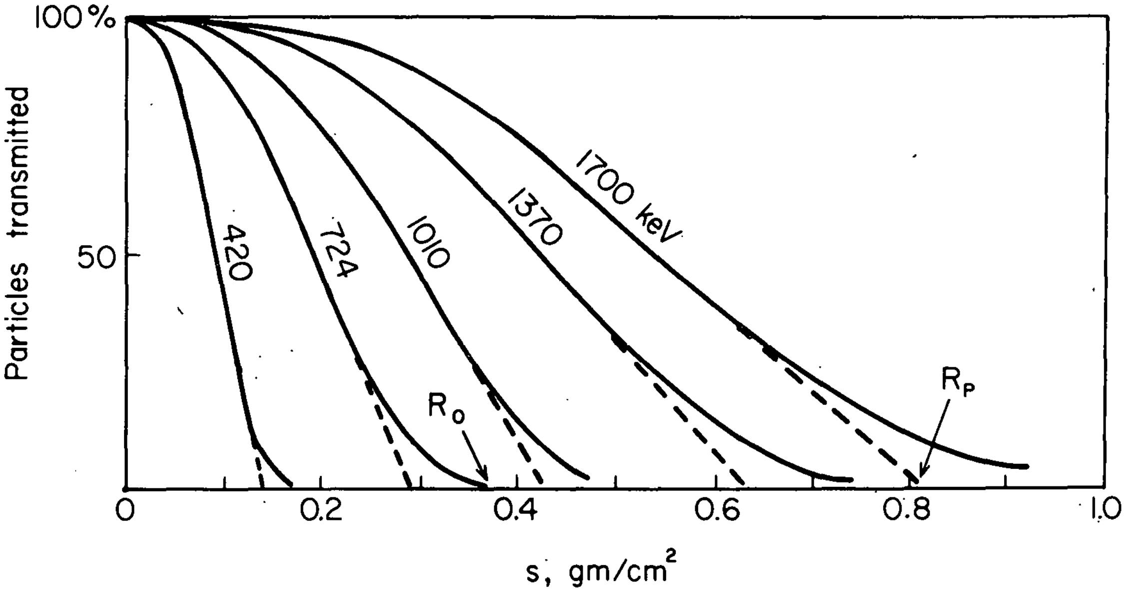

XBL 696-657

Fig. 12. Absorption curve of mono-energetic electrons. R_p is defined as the extrapolated range, R_o as the maximum range (BK58).

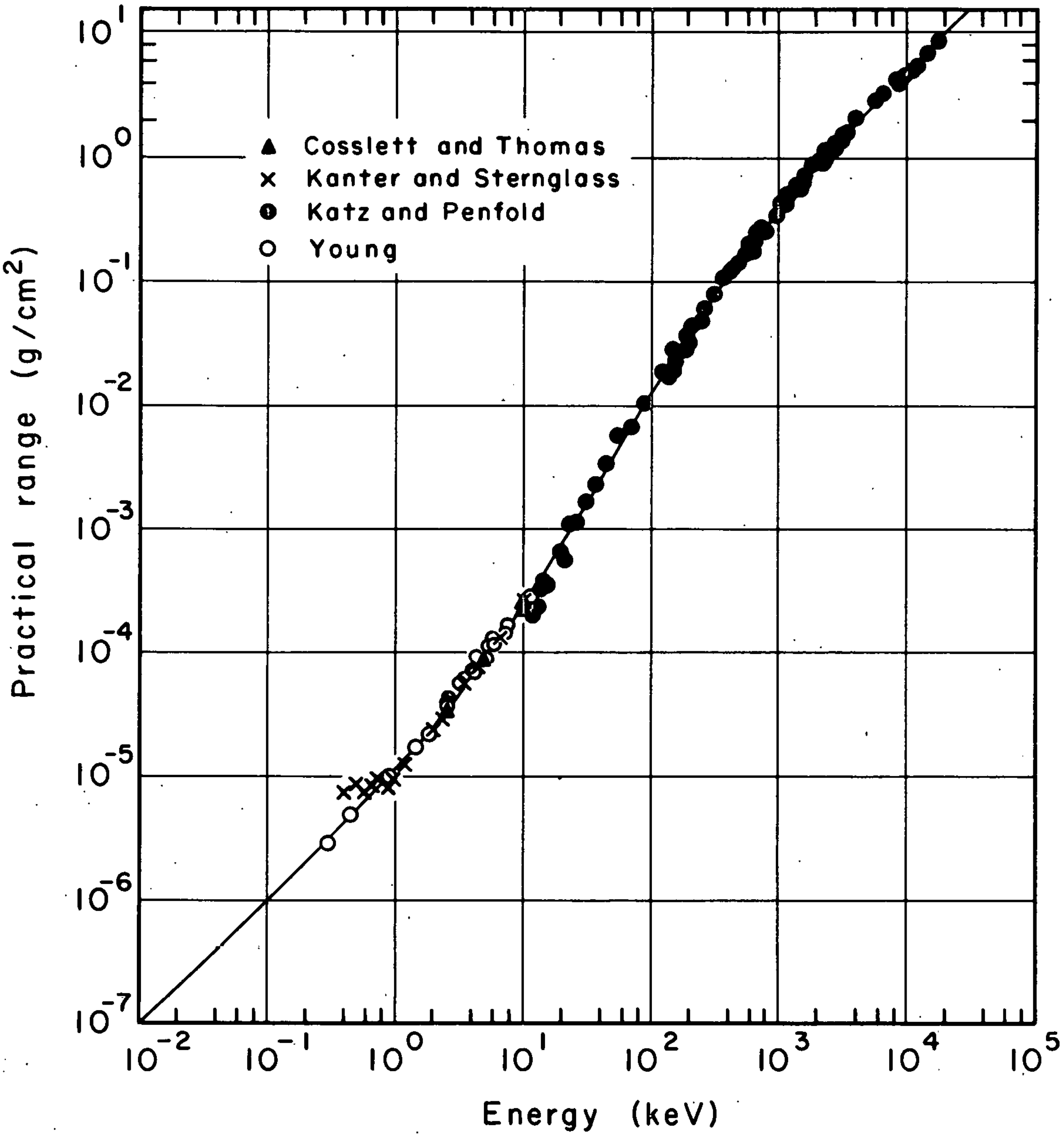

XBL695-2765

Fig. 13. Practical range in aluminum versus electron energy (KK68). Coslett and Thomas (CT65); Kanter and Sternglass, Phys. Rev. 126, 620 (1962); Katz and Penfold (KP52); Young, Phys. Rev. 103, 292 (1956).